

2-P (mix)

NASA CR-130111

NTIS \$6.75

STAR

HS324-5214

MULTISPECTRAL SCANNER SYSTEM FOR ERTS

FOUR BAND SCANNER SYSTEM

NASA Contract NAS 5-11255

SPACE AND COMMUNICATIONS GROUP
HUGHES AIRCRAFT COMPANY
EL SEGUNDO, CALIFORNIA

**ORIGINAL CONTAINS
COLOR ILLUSTRATIONS**

August 1972

FINAL REPORT

VOLUME II
ENGINEERING MODEL
PANORAMIC PICTURES AND
ENGINEERING TESTS

Prepared for:
GODDARD SPACE FLIGHT CENTER
GREENBELT, MARYLAND 20771

Reproduced by
**NATIONAL TECHNICAL
INFORMATION SERVICE**
U.S. Department of Commerce
Springfield, VA. 22151

(NASA-CR-130111) MULTISPECTRAL SCANNER
SYSTEM FOR ERTS: FOUR BAND SCANNER
SYSTEM. VOLUME 2: ENGINEERING MODEL
PANORAMIC PICTURES AND (Hughes Aircraft
Co.) Aug. 1972 93 p CSCL 14B



G3/14

Unclas
49449

N73-14430

SCG 20529R

TECHNICAL REPORT STANDARD TITLE PAGE

1. Report No. HS 324-5214	2. Government Accession No.	3. Recipient's Catalog No.	
4. Title and Subtitle MULTISPECTRAL SCANNER SYSTEM FOR ERTS Four Band Scanner System		5. Report Date September 1972	
		6. Performing Organization Code	
7. Author(s)		8. Performing Organization Report No.	
9. Performing Organization Name and Address Hughes Aircraft Company Space and Communications Group 1950 E. Imperial Highway El Segundo, California		10. Work Unit No.	
		11. Contract or Grant No. NAS 5-11255	
12. Sponsoring Agency Name and Address National Aeronautics and Space Administration Goddard Space Flight Center Greenbelt, Maryland 20771		13. Type of Report and Period Covered Final Report, Vol. II	
		14. Sponsoring Agency Code	
15. Supplementary Notes			
<p>16. Abstract</p> <p>This document is Volume II of three volumes of the Final Report for the four band Multispectral Scanner System (MSS). Contained herein is the results of an analysis of pictures of actual outdoor scenes imaged by the engineering model MSS for spectral response, resolution, noise, and video correction. Also included are the results of engineering tests on the MSS for reflectance and saturation from clouds. Finally, two panoramic pictures of Yosemite National Park are provided in Appendix C.</p> <p style="text-align: center;">ORIGINAL CONTAINS COLOR ILLUSTRATIONS</p>			
17. Key Words (Selected by Author(s)) Multispectral Scanner System (MSS) Panoramic Pictures by MSS MSS Engineering Model Tests		18. Distribution Statement	
19. Security Classif. (of this report) UNCLASSIFIED	20. Security Classif. (of this page)	21. No. of Pages 93	22. Price*

INTRODUCTION

The Final Report for the Multispectral Scanner System (MSS) Program is provided in two portions. The first portion is written at the conclusion of the 4-band program, and the second portion will be written subsequent to completion of the 5-band program.

The 4-band final report is in three volumes. The first volume describes the system and compares its performance with the original objectives. The second volume describes some field experiments performed at the end of the program using the engineering model scanner and multiplexer. Volume III will be an analysis of in-orbit performance and will be written later.

This document is Volume II. It contains data on the response of the scanner to different terrains, vegetation, and lighting conditions (Chapter 1); an estimate of vertical and horizontal resolution using known objects such as buildings (Chapter 2); an analysis of linear mode and compression mode effects on picture quality (Chapter 3); a description of the experience gained in using ground truth information for video correction (Chapter 4); an analysis of the effects of adding known levels of noise simulating microphonics, coherent noise, and random noise (Chapter 5); a comparison of natural photographic false color and MSS false color (Chapter 6); and data and evaluation of reflectance tests (Chapter 7). Appendix A gives a complete inventory of the scenes imaged by the engineering model. Appendix B describes a test which determined the effect on the scanner of saturation from clouds. Finally, Appendix C presents two panoramic pictures of Yosemite National Park taken by the engineering model MSS.

Laboratory testing of the MSS exercised almost every operational facet of the system, except the response to a reflected solar spectrum and the resolution in the direction across scan lines. Since the solar spectrum is difficult to simulate within a laboratory, it was decided to scan actual outdoor scenes using the engineering model. The scenes were selected for variety and for situations which permit relatively long ranges. The latter is desirable because the hyperfocal distance for the scanner is on the order of 7 miles and scenes at closer distances become increasingly blurred. The important limitation of these scenes is that the ERTS imaging will give views of the earth from 496 n.mi., which are not as detailed as the ground-based views obtained in this test. When examining spectral characteristics of a tree in these scenes, it is necessary to substitute, mentally, an acre of homogeneous trees.

The engineering model configuration was modified by incorporating the flight unit power supply changes. The engineering model performance is therefore expected to be very close to that of the flight equipment.

To permit careful analysis, the first 20 copies of this volume contain glossy photographs for the panoramic pictures in Appendix C. For purposes of economy, the remaining copies of this volume contain halftone reproductions of these pictures.

**Details of illustrations in
this document may be better
studied on microfiche**

**COLOR ILLUSTRATIONS REPRODUCED
IN BLACK AND WHITE**

CONTENTS

	Page
1. AN EXAMPLE OF THE OPERATIONAL USE OF MSS PICTURES	1-1
1.1 Operational Use of MSS	1-1
1.2 Example	1-1
2. VERTICAL AND HORIZONTAL RESOLUTION EVALUATION AND REGISTRATION	2-1
2.1 Vertical and Horizontal Resolution Evaluation	2-1
2.2 Registration	2-4
3. LINEAR/COMPRESSION QUANTIZATION EFFECTS ON PICTURE QUALITY	3-1
3.1 Definition of Density	3-1
3.2 Quantization Effects on Density	3-2
3.3 Actual Scene Results	3-2
4. VIDEO CORRECTION EVALUATION	4-1
4.1 First Video Correction of Scenes	4-1
4.2 Initial Video Correction Attempt With Flooding Lamp Data	4-1
4.3 Use of Nominal Gray Wedge	4-1
4.4 Use of Image Data	4-2
4.5 Computation Procedure	4-3
4.6 Results	4-4
4.7 Computation of Relative Gains	4-6
4.8 Stability of Calibration System	4-7
4.9 Summary	4-8
5. EFFECTS OF INTERFERENCE PHENOMENON ON SCENE INFORMATION	5-1
5.1 Test Sites and Mode	5-1
5.2 Microphonics and Coherent Noise Test	5-1
5.3 Random Noise Test	5-1
5.4 Results	5-4

6.	EVALUATION OF FALSE COLOR COMPOSITE IMAGES AS PRODUCED FROM MSS IMAGERY	6-1
6.1	Assignment of Colors to Bands	6-1
6.2	Effect of Color Assignments on Scene Objects	6-1
6.3	Color Processing Problems	6-2
6.4	Film Dyes	6-2
7.	REFLECTANCE TESTS	7-1
7.1	Measurements of Scanner	7-1
7.2	Measurements of Sun	7-4
7.3	Apparent Reflectance Calculation	7-4
7.4	Predicted Signals	7-6
7.5	Conclusions	7-6
7.6	Derivation of Scanner Response	7-9
APPENDICES		
A.	Picture Sites	A-1
B.	Engineering Model Cloud Test	B-1
C.	Yosemite Panoramic Scenes	C-1

1. AN EXAMPLE OF THE OPERATIONAL USE OF MSS PICTURES

1.1 OPERATIONAL USE OF MSS

Imagery will be used for examining rock structure, locating ore, oil, and other mineral deposits, making land use surveys for water control, and other applications that are expected to arise as the pictures become available to a wide audience. The usefulness for these applications will depend upon the "crispness" of the images, which is specified in terms of MTF.

Data in quantized form can be compared on a band-to-band basis to assist in forestry and crop inventories. Users may be expected to discover other applications after they become accustomed to data of this type. The value of the MSS for this type of analysis depends upon the radiometric accuracy which was demonstrated primarily by laboratory testing; however, the outdoor pictures demonstrate the spectral balance and the specialized response of band 3 to growing material.

1.2 EXAMPLE

The earth scenes afford some examples of the multispectral effects which influenced the selection of a broadband scanner for earth resources imaging. Subtle distinctions in which growing materials are identified will require comparison of the quantized signal levels from band to band. Grosser variations can be discerned by means of the "false color" technique. In Figure 1-1, the growing materials appear in red and pink hues because they are highly reflective in band 3 which has been assigned the color 'red' in the composite. Some trees have begun to lose their vigor and appear to be brown. This effect occurs in band 3; whereas, the loss in reflectivity is not apparent in the green band (band 1) until the decrease is well established.

Figures 1-2 and 1-3 are examples of trees imaged simultaneously in bands 1 and 4. Several of the trees stand out in band 4 because of lowered reflectivity. The same trees can be seen to be darker also in band 1;

however, the eye is guided to these after spotting them first in the near IR band. It is planned that this sensitivity of the IR band to decline of growing materials at the early stages can be used to identify diseased parts of forests in sufficient time to prevent spreading to the entire forest.

A trend that can also be seen in these two frames of Lake Tahoe is the clarification of a patch of ground designated by circles on the overlays in bands 1 and 4, respectively. Band 1 gives little differentiation between this and the adjacent foliage; whereas, the darker flat quality in band 4 gives a good indication of bare ground.

Reproduced from
best available copy.



20529-1(U)

Figure 1-1. Half Dome at Yosemite National Park

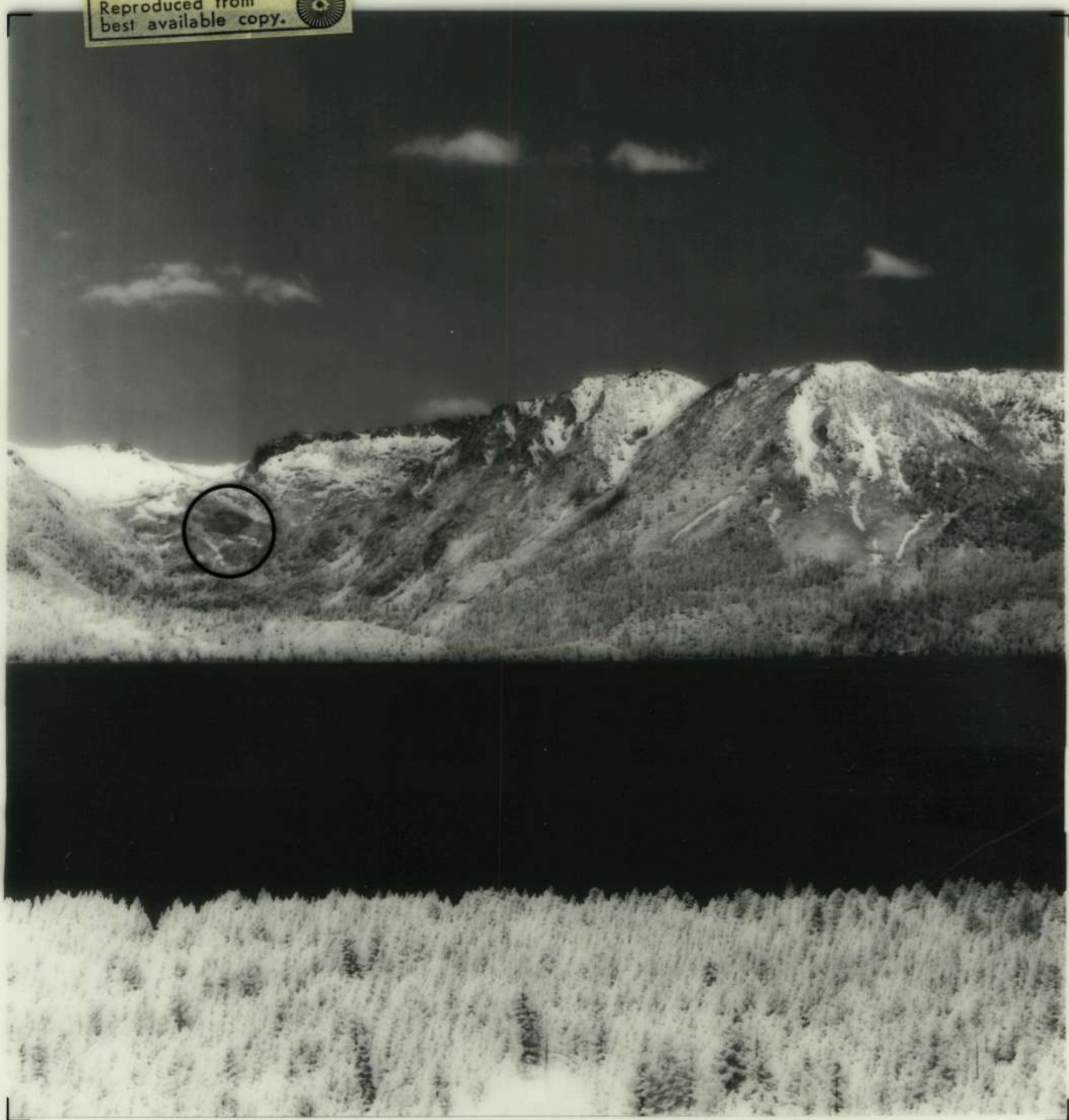
Reproduced from
best available copy.



1-3-a

Figure 1-2. Band 1 Image of Lake Tahoe Area

Reproduced from
best available copy.



1-H-a

2. VERTICAL AND HORIZONTAL RESOLUTION EVALUATION AND REGISTRATION

2.1 VERTICAL AND HORIZONTAL RESOLUTION EVALUATION

2.1.1 Photographic Dimensions Subtending Field Stop Angle

It is convenient to have a measure of the dimension which represents an instantaneous field of view (IFOV) for the scanner. The FOV of 11.6 degrees (100 n.mi. in operation) is reproduced here in the GPE format of 7.25 inches, which means that the IFOV of 67 microradians for the engineering model* subtends 0.0024 inch on the picture. This can be applied to objects in the picture regardless of the range of the object, so that any element having a dimension of 2.4 milli-inch (61 mm) subtends 67 microradians, or an IFOV. Figure 2-1 shows a plot of feet subtended by the IFOV as a function of distance from the scanner.

2.1.2 Scene Examples of Resolution Capability

Transparencies give a much crisper scene than can be expected from any print and, especially, reproductions of prints. Therefore, the transparencies used to assess resolution are reproduced here. In analyzing the transparency for the San Francisco scene (Figure 2-2), a few buildings have horizontal partitions between floors which were found to have a thickness of one IFOV (0.0024 inch). An example is the white building next to the Mark Hopkins, which has a range of about 4.4 miles. This represents a response along scan of 1.7 feet or a resolution of 203 feet from ERTS. The response in this direction is influenced by field stop, blur circle, electrical filter, line-to-line alignment, data sampling, and photographic processing.

Examples in the scene which demonstrate the resolution perpendicular to the scan direction are harder to find. However, the vertical separations between windows of the Fairmont Hotel in the San Francisco skyline subtends 0.1 mm, which corresponds to 2.8 feet at the range of 4.4 miles. This represents a resolution of 220 feet under ERTS conditions. Resolution in this direction is a function of blur circle, line-to-line spacing, field stop, and scan accuracy.

* This represents the field stop(S) formed by the optical fiber core. The engineering model is slightly smaller than flight models. (S = 0.0023 inch, focal length = 33.2 inches).

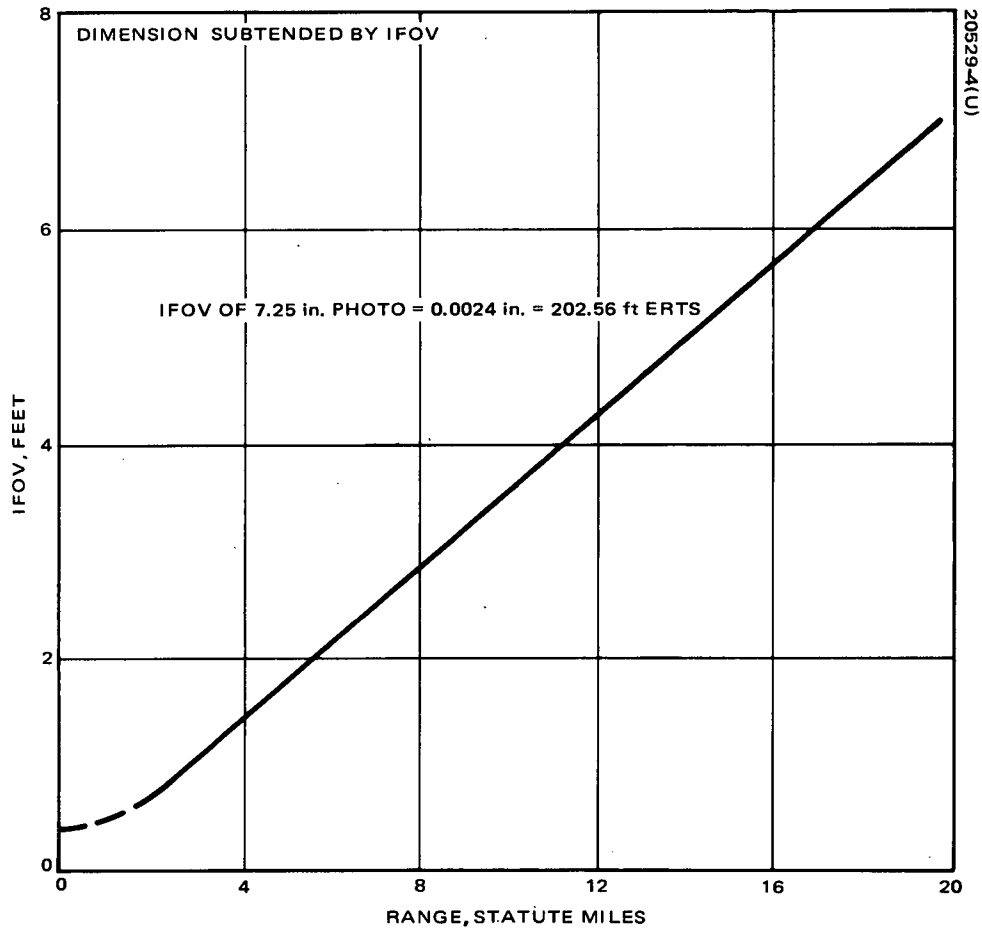
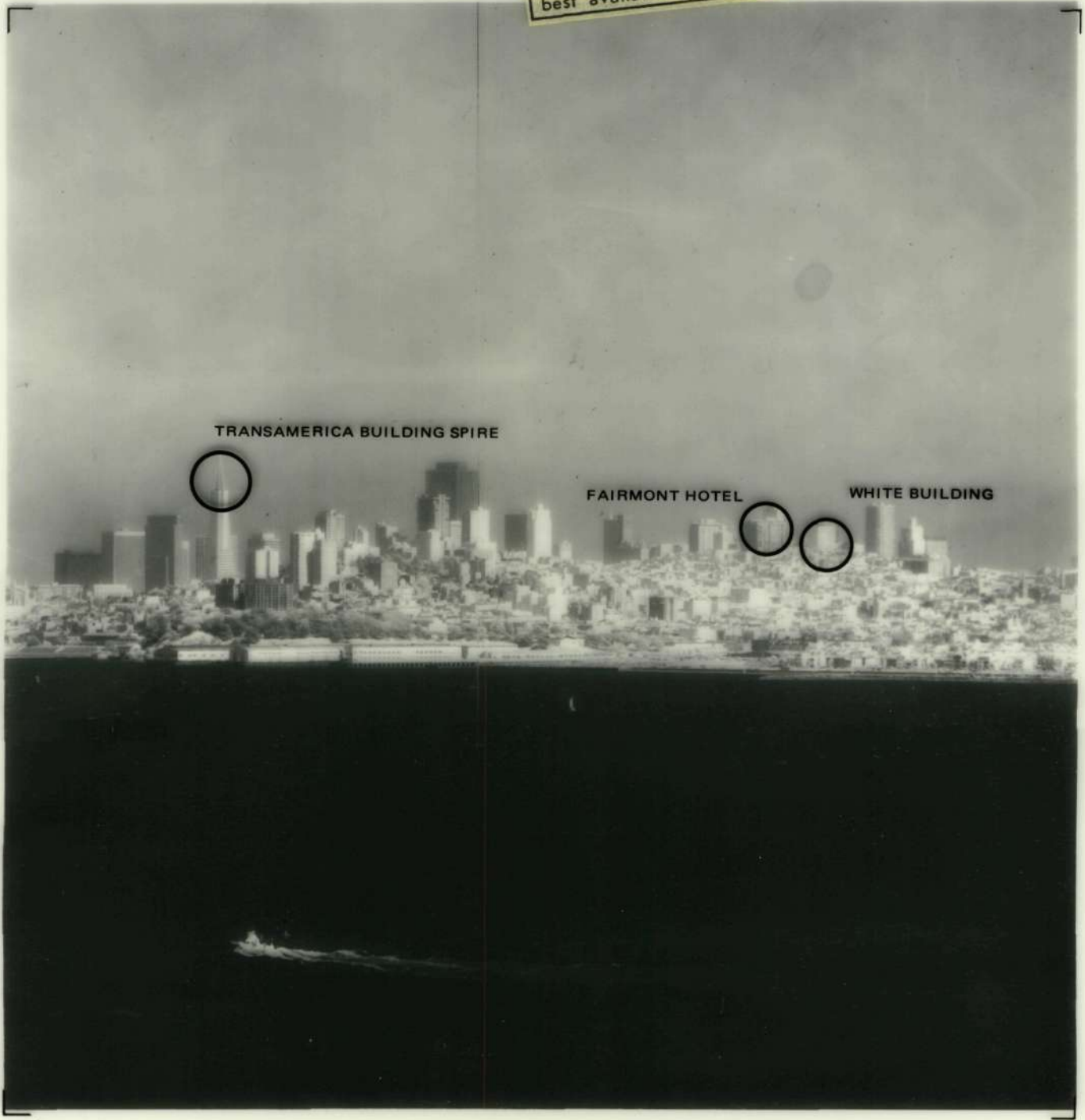


Figure 2-1. MSS Engineering Model IFOV Versus Range

Figure 2-2. Band 2 Image of San Francisco Skyline

Reproduced from
best available copy.



TRANSAMERICA BUILDING SPIRE

FAIRMONT HOTEL

WHITE BUILDING

2-3a

A numerical assessment is difficult to achieve in these "targets of opportunity"; however, such examples as the architectural separators bear out the analysis made early in the program in which the vertical and horizontal MTFs were calculated to be nearly equal.*

An example of a known dimension can be seen in the supports which make up the spire that surmounts the Transamerica Pyramid. Figure 2-3 is a schematic drawing of the spire. The triangular frame consists of square columns with sides of 2 feet which have an apparent width of 2.8 feet at the angle viewed. Since the distance is 4.72 miles, this translates into 1.7 IFOVs or 0.004 inch (0.1 mm). The angle at which the picture was taken in relation to the building and its surroundings is given in the figure.

Table 2-1 summarizes the resolution estimates converted to ERTS operational conditions.

TABLE 2-1. ESTIMATED RESOLUTION PARALLEL AND PERPENDICULAR TO SCAN LINES FROM MSS ENGINEERING MODEL PICTURES

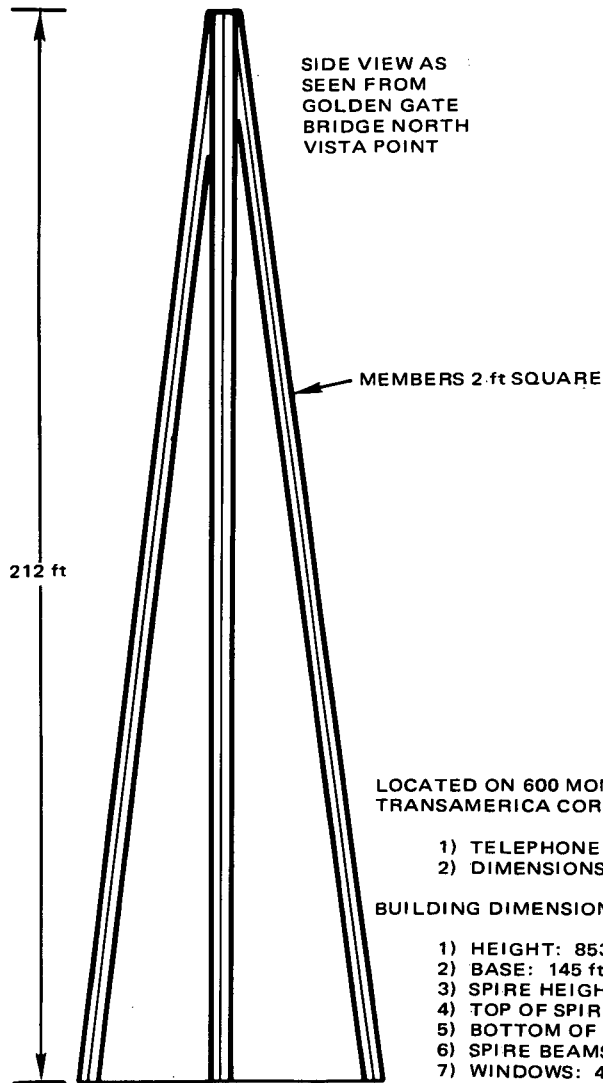
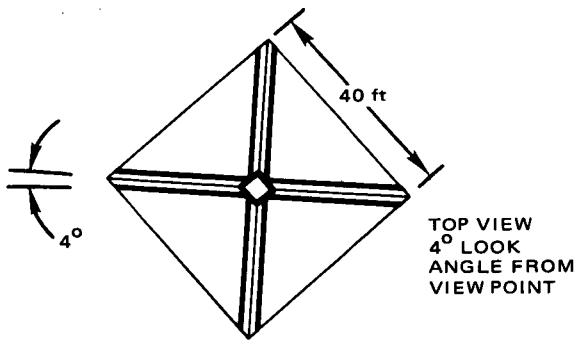
Parameter	Engineering Model	Prototype/ Flight A
Design resolution, feet	203	225
Parallel to scan, feet	203	225
Perpendicular to scan, feet	220	245

Resolution estimates made from San Francisco skyline buildings.

2.2 REGISTRATION

The fiber spacings in the focal plane were selected in conjunction with the mechanism scan rate and sampling rate, so that the n^{th} sample in band 1 corresponds to the $n + 2$ sample in band 2, $n + 4$ sample in band 3, and $n + 6$ sample in band 4. The coincidences are very slightly disturbed by the mild variation from a constant scan rate and the degree to which the fiber matrix is misaligned. The combined effect of these factors could amount

*II System Engineering Section. Concepts Review Package.



LOCATED ON 600 MONTGOMERY STREET BETWEEN CLAY AND WASHINGTON
TRANSAMERICA CORPORATION DEVELOPERS AND BUILDERS.

- 1) TELEPHONE 982-2330
- 2) DIMENSIONS ON BUILDING SUPPLIED BY BILL ANDERSON, ARCHITECT.

BUILDING DIMENSIONS.

- 1) HEIGHT: 853 ft
- 2) BASE: 145 ft SQUARE (STARTS AT 5th FLOOR)
- 3) SPIRE HEIGHT: 212 ft
- 4) TOP OF SPIRE: 4 ft SQUARE
- 5) BOTTOM OF SPIRE: 40 ft SQUARE
- 6) SPIRE BEAMS: 2 ft SQUARE
- 7) WINDOWS: 4 ft 10 in. x 6 ft HIGH

Figure 2-3. Spire Top of Transamerica Pyramid Building
in San Francisco

to misregistration of 50 feet between channel 2 lines of bands 1 and 4. This statement pertains to the sample coincidence as used by the computer in signature analysis. The registration of the photographs does not suffer from the changes in scan rate, since one can interpolate between samples, which is the effect of sliding the pictures across each other.

Two spectral bands for the San Francisco skyline scene were examined for registration by sliding the transparencies until the scene was optimally aligned when viewed through an X7 magnifying glass. The fiduciary marks were then found to be exactly superimposed. The architectural divisions described in subsection 2.1 were then re-examined with a scaled magnifier and no deterioration in the edges or width of one IFOV could be discerned. This indicates that the resolution is not depreciated by registration errors. This is the primary measure of excellent registration.

3. LINEAR/COMPRESSION QUANTIZATION EFFECTS ON PICTURE QUALITY

3.1 DEFINITION OF DENSITY

When the scanner signals are processed into pictures, the following general function is used to reproduce the scene as viewed by the scanner:

$$\text{Density} = \text{minimum density} + (\text{gamma}) \log \left(\frac{\text{volts output}}{\text{full scale volts}} \right)$$

or

$$D = D_{\min} + G \log (V_o / V_{\max})$$

where for

Positive transparencies, $G = (-G)$

Negative transparencies, $G = (+G)$

V_o = the scanner output scene voltage

V_{\max} = the maximum scanner output, 4 volts

The gamma for normal reproduction of scene data is one, but can be any desired function for enhancing different portions of the scene. The D_{\min} is the minimum film density desired and is usually set from a density of 0.1 to 0.2 above the film fog level. The MSS GPE use a D_{\min} of 0.3.

Examination of the function above reveals that the basic relations between the density on the film and scene brightness, scanner output voltage, is logarithmic; i.e.,

$$D \cong \log (I \text{ or } V)$$

Since the eye is also logarithmic in distinguishing steps, the eye perceives density steps linearly, whereas equal light levels appear too coarse at low levels and are wasted at high levels. Therefore, more visual information can be transmitted by equalizing the density steps, not the light level steps.

3.2 QUANTIZATION EFFECTS ON DENSITY

Figures 3-1 and 3-2 are provided to illustrate the density effects in the MSS linear and compression modes. To simplify the drawings, they are given for 16 levels over the range of 0 to 4 volts (the MSS System has 64 levels over the range).

Figure 3-1a illustrates linear mode quantization where unequal density levels result from equal light level quantization. This results in coarser density levels at low light scenes. Figure 3-1b illustrates the improvement in equalization of density levels which result from the use of compression. In this case, the analog data has been modified by the multiplexer compression characteristic and this characteristic has been removed in the GPE digital processor. The resulting GPE film has density levels which are more nearly equal (i.e., more levels (finer sampling) is provided at low light inputs, and somewhat coarser sampling (less levels) at higher light levels).

Figure 3-2 illustrates the effect of encoding with the compression mode in the flight subsystem, and ground processing the data as if it were linearly encoded. This results in a contrast enhancement effect on low light level scenes, where more finely spaced quantization with somewhat larger density steps are achieved. However, this is accomplished at the expense of less density steps at higher light level scenes.

Where only a few density steps occur over a large voltage range, the result is a contouring effect in the output GPE pictures. Thus, for linear quantization (Figure 3-1a), four density levels are achieved between 0 and 1 volt, while in compression quantization, (Figure 3-1b), six levels result. Where quantization is not removed in ground processing (Figure 3-2), seven levels result. Contouring (in the 0 to 1 volt range) would be more severe in the linear case and less severe when compression is used.

3.3 ACTUAL SCENE RESULTS

The Lake Tahoe and Yosemite pictures were taken in both linear and compression modes. Examination of these pictures showed a slight improvement in low level scene detail and contouring in the compression mode. Furthermore, a slight increase in video striping was observed in the linear mode pictures.

When the compression mode pictures were processed using linear video correction, greater detail in low level scenes and contouring was evident.

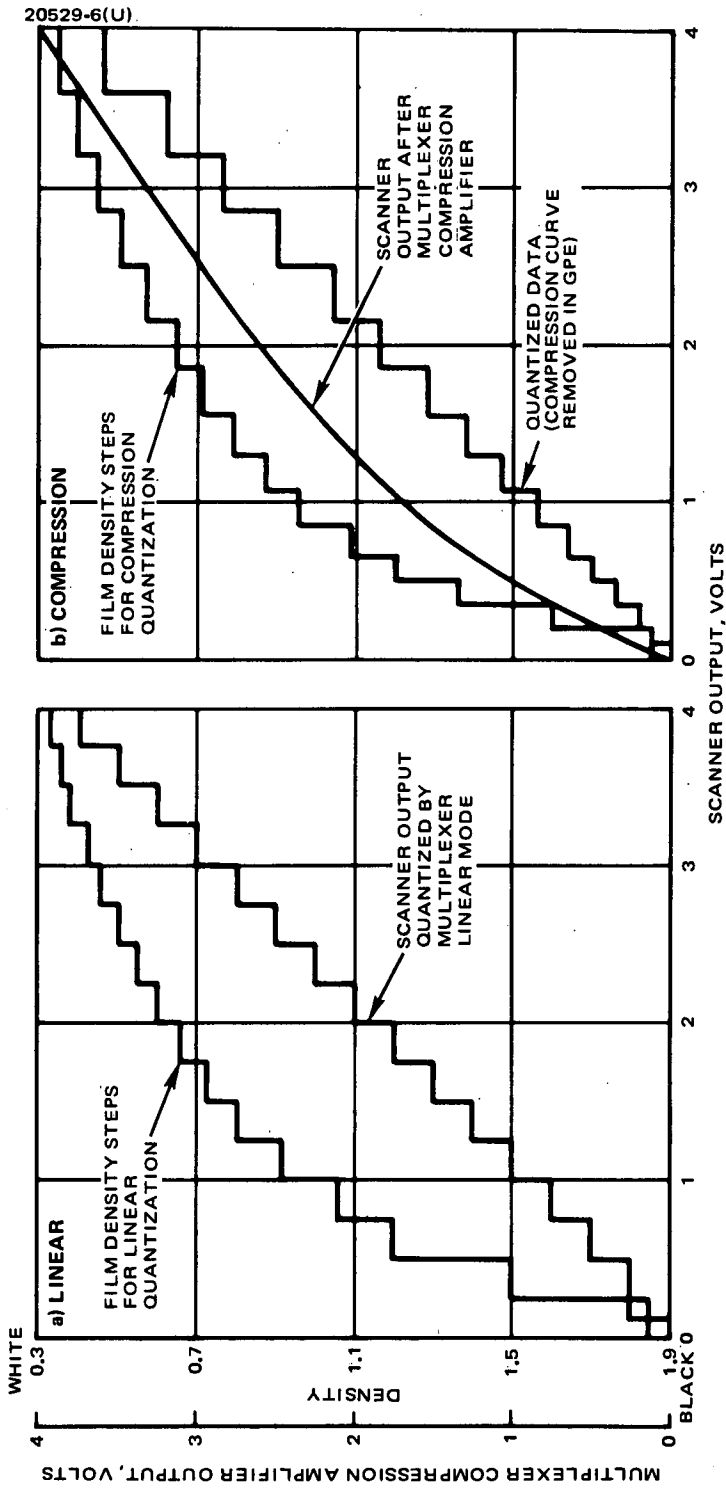


Figure 3-1. MSS Linear/Compression Mode Picture Quantization Comparison

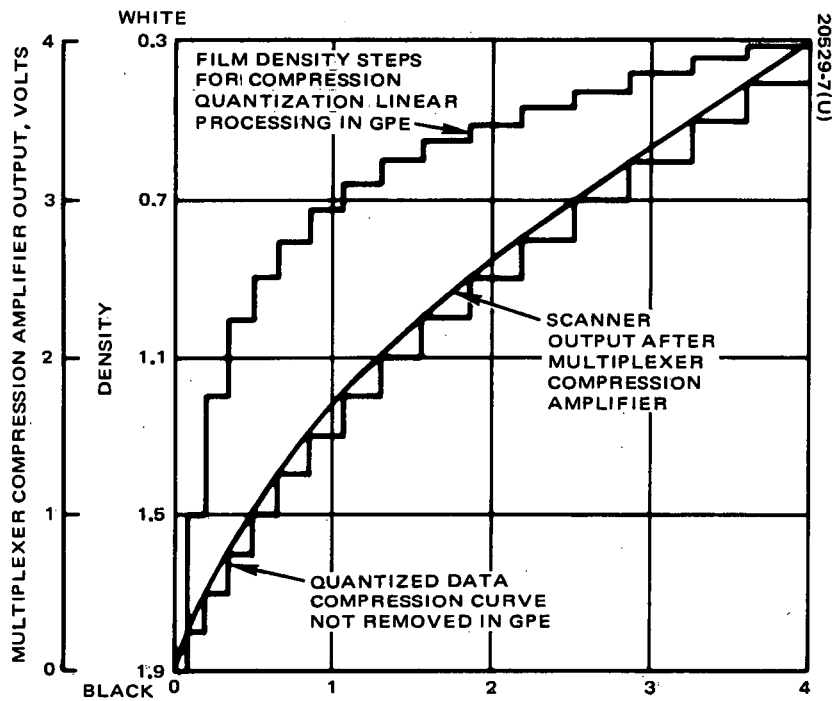


Figure 3-2. MSS Compression Mode Enhancement

4. VIDEO CORRECTION EVALUATION

4.1 FIRST VIDEO CORRECTION OF SCENES

The first effort at video correction of scenes was the destripping of the first tapes made at Santa Barbara. Here the sky was used as a reference in bands 1 and 2 and the out-of-focus foreground as a reference in bands 3 and 4. No offset correction was made. The results were generally excellent. However, the scenes did not contain any extended dark areas which would reveal offset errors.

4.2 INITIAL VIDEO CORRECTION ATTEMPT WITH FLOODING LAMP DATA

The tapes of scenes taken across California all included a flooding lamp calibration sequence. Theoretically, it should be possible to obtain both gain and offset from these images. The first attempt at this type of data reduction was made with tape 7, Meeks Bay, in Lake Tahoe. This tape was chosen because the scene on it contained both high light levels (snow and sky), and water, which is quite dark and nearly uniform.

The first calculation using flooding lamp data showed offsets in bands 1, 2, and 3 on the order of -8 to -10 quantum levels. This was so high that it was concluded that something was wrong with the image data (lamp movement, for example).

Repeating this calculation with tape 5, Kingsbury Grade, Lake Tahoe, gave offsets which were far more reasonable, but still highly suspect. The flooding lamp was then abandoned as a source of calibration information.

4.3 USE OF NOMINAL GRAY WEDGE

Sixty-four level gray wedge measurements were made in the flooding lamp portions of tape 7, Meeks Bay. These gray wedges were used to develop eight-level nominal gray wedges, using the techniques developed during the flight A thermal vacuum tests. The eight sample points were bunched rather than being evenly distributed throughout the gray wedge. The PMT bands had two high level sample points and six low level sample points. The diode band used four high level sample points and four low level

sample points. The initial intent was to use the flooding lamp data to provide offset correction data for these nominals. As the flooding lamp data was now suspect, the gray wedge levels were assigned zero offset.

The first attempt to use the nominal gray wedge tables was disappointing. Although the gray wedge program yielded sensible results in the flooding lamp portion of tape 7, the scene portions of the tape yielded offsets of -5 to -10 quantum levels. In addition, the measured gray wedge values had sunk to such an extent in the scene portion of the tape that most, and in some cases, all six of the low level data points were below quantum 3 and, therefore, discarded by the gray wedge program. New word counts were chosen and new nominals calculated. The result was still offsets in the -5 to -10 quantum level area for bands 1, 2, and 3. Only the band 4 offsets were small and nearly reasonable. The new nominals run against tape 5, Kingsbury Grade, were essentially the same. In addition, it was noticed that the fit in both tapes 5 and 7 was very poor. Individual points showed as much as a 2 quantum level error compared to the least squared fit straight line. The conclusion drawn at this point was that the tape 7, Meeks Bay, flooding lamp data suffered from a serious and mysterious defect and something else would have to be done. Later it was found that low ambient temperatures had upset the prime power generator and the resulting low line voltage was causing large offsets and nonlinear operation in the scanner.

4.4 USE OF IMAGE DATA

At this point a week of effort had been invested and there was very little to show for it. Meeks Bay flooding lamp data was unusable, and by extrapolation another week might be spent with another tape studying the flooding lamp data with little progress achieved. Therefore, it was decided to see what could be done to obtain the necessary information from image data. In theory, if there are two scenes, one bright and the other dark, a calculation can be made for relative gain and relative offset for each sensor which will result in a stripe-free GPE picture of both scenes. Both the Meeks Bay (tape 7) and Kingsbury Grade (tape 5) tapes contained both sky and water scenes, but because of the tape 7 anomalies, tape 5 was used for further work.

First, a new set of nominals was obtained. This was done by picking a set of word counts which were not likely to be clipped (i. e., levels less than 60 and greater than 8). These were programmed into the computer without regard to the associated nominal levels, and the gray wedge program was run for all 24 channels at 2100 feet, tape 5. The resultant measured values were then transferred to the nominal table. Therefore, gain and offset in all other tapes would be measured relative to 2100 feet, tape 5.

Next, steady-state, signal-to-noise, and gray wedges were obtained for both sky and water in all 24 channels. This data set provided the information necessary to determine the relative channel-to-channel gains (i. e., photo equalization factors) and the channel-to-channel offsets. Absolute

offset could not be determined; however, this is essential only for radiometric calibration and is not absolutely essential in making a satisfactory GPE picture.

4.5 COMPUTATION PROCEDURE

The computation of photo equalizations and relative offset from two level scene data is performed as follows. The ratio between the corrected signal levels for the two scenes will be the same when the correct relative offsets and photo equalization factors are determined; that is:

$$\text{CORSIG} = \frac{Q_{\text{ch}} + 0.5 - \emptyset_{\text{ch}}}{(G_{\text{ch}}) (\text{EQPH}_{\text{ch}})}$$

where

CORSIG = the corrected signal level

Q_{ch} = the measured signal level

\emptyset_{ch} = the true offset

G_{ch} = $1 + \Delta G$; i. e. the gain relative to the nominal gain for that channel

EQPH_{ch} = photo equalization factor for the channel.

Next, define

$$R_{\text{ch}} = \frac{\text{CORSIG}_{\text{ch}}}{\text{CORSIG}'_{\text{ch}}}$$

where

R_{ch} = ratio between the low light level scene CORSIG' and the high level scene CORSIG

Now $R_1 = R_2 = R_3 \dots = R_{\text{Band}}$ and if R_{Band} is known, the true offset can be determined. Unfortunately, R_{Band} cannot be determined with the available data set. Nevertheless, a solution can be obtained if it is assumed that the band average offset is near zero or if R_{Band} is taken to be equal to the band average of the ratios R_{ch} obtained using the best available offset data. The result will not be the true offset, but will reflect the channel-to-channel offset. These offsets, when used in picture processing, will yield a stripe-free picture which, in general, if the offsets are small, will be indistinguishable from one in which the density versus light level relation is exact. Therefore, let $\emptyset M_{\text{ch}}$ be the best estimate of the channel offset. Then, R_{Band} may be defined as:

$$R_{\text{Band}} = \left[\frac{6}{\pi} \left(\frac{(Q_{\text{ch}} + .5 - \emptyset M_{\text{ch}}) G'_{\text{ch}}}{(Q'_{\text{ch}} + .5 - \emptyset M'_{\text{ch}}) G_{\text{ch}}} \right) \right]^{1/6}$$

where the unprimed and primed values are from the first and second scene, respectively.

Then, the channel-to-channel offset error in the measured offset QM is:

$$E_{\text{ch}} = \frac{(Q_{\text{ch}} + .5 - \emptyset M_{\text{ch}}) G'_{\text{ch}} - R_{\text{Band}} (Q'_{\text{ch}} + .5 - \emptyset M'_{\text{ch}})}{G'_{\text{ch}} - (R_{\text{Band}}) (G_{\text{ch}})}$$

and the offset value which will destripe the picture is given by:

$$\emptyset_{\text{ch}} = \emptyset M_{\text{ch}} - E_{\text{ch}}$$

This technique was used to develop the photo equalization factors and offset corrections for 2200 feet, tape 8 (Golden Gate), 2100 feet and 6130 feet, tape 5 (Kingsbury Grade), and 2300 feet, tape 7 (Meeks Bay).

4.6 RESULTS

The results are shown in Table 4-1. The average offset correction shown in the table was then used to correct the gray wedge readings for all other tapes. It must be kept in mind that Table 4-1 represents the offsets which existed at the time the gray wedge levels were chosen (i. e., 2200 feet, tape 5, Kingsbury Grade). Because the gray wedge nominal levels were taken to be equal to the levels found at 2200 feet in tape 5, the

TABLE 4-1. WEDGE OFFSET CORRECTIONS USING
TWO SCENE LEVELS

Tape - 8.2200 Golden Gate						
Band	Offsets By Channel					
1	-0.312	0.811	1.163	-0.093	-0.201	-1.165
2	0.288	-0.312	-0.767	0.381	0.173	0.455
3	0.241	-0.084	-0.161	-0.319	0.524	-0.177
4	-0.763	0.849	1.071	-0.733	1.392	-0.587
Tape - 5.6130 Kingsbury Grade						
1	-0.255	0.677	1.138	-0.250	-0.036	-1.108
2	0.373	-0.187	-0.927	0.196	0.252	0.468
3	0.264	-0.063	-0.351	-0.102	0.499	-0.230
4	-0.904	0.942	0.951	-0.858	1.137	-0.609
Tape - 5.2100 Kingsbury Grade						
1	-0.112	0.834	0.866	-0.102	-0.297	-1.093
2	0.093	-0.146	-0.893	0.476	0.221	0.423
3	0.222	-0.116	-0.327	-0.247	0.514	-0.046
4	-0.745	0.915	0.925	-0.823	1.006	-0.724
Tape - 7.2300 Meeks Bay						
1	-0.230	0.698	0.986	-0.006	-0.295	-1.001
2	0.319	-0.222	-0.938	0.272	0.170	0.697
3	0.173	0.092	-0.254	-0.233	0.479	-0.198
4	-0.660	1.016	0.928	-0.792	1.199	-0.443
Average Values						
1	-0.227	0.755	1.038	-0.113	-0.207	-1.092
2	0.268	-0.217	-0.881	0.331	0.204	0.511
3	0.225	-0.043	-0.273	-0.225	0.504	-0.163
4	-0.768	0.931	0.969	-0.801	1.184	-0.591

delta gain and offset obtained from the Honeywell 516 gray wedge program will both be zero. The average offsets shown in Table 4-1 are therefore the values which must be added to the computed offset to obtain the true offsets. After this, basic calibration data reduction on all other tapes involved first obtaining gray wedge gain and offset using the Honeywell 561, and then adding the offset corrections to the measured offsets.

The result of the above technique was generally excellent as far as offsets are concerned. Bands 3 and 4 are free of low level striping (offset error) except for Yosemite, where traces of striping are found in extreme shadows in some band 3 pictures and one band 4 picture. This striping may be due to quantization limitations. Band 2 showed consistent moderate striping at low levels (offset error) in all pictures except for a few made from tape 5. A recheck of the data and programs disclosed a typographical error whereby the offset correction for sensor 10 was entered as -0.331 instead of +0.331 quantum levels. The resultant 2/3 quantum level offset error is clearly visible in the shadow area of most band 2 pictures. Band 1 was generally excellent, but occasionally has light striping in shadows.

Throughout the tapes, the offsets were fairly consistent for any one location; changing locations produced up to ±0.45 quantum level shift. The noise level in the measurements is estimated to be ±0.1 quantum level.

4.7 COMPUTATION OF RELATIVE GAINS

The computation of channel-to-channel relative gains was broken into two steps. The first step was the computation of the change in the individual channel gain from the gain it exhibited at 2100 feet in tape 5. This number is obtained directly from the Honeywell 516 gray wedge program. This number would contain both the actual gain change and any error due to a change in the calibration system.

The next step was computation of the photo equalization factors. Using various "truth" sites in the scene data (typically a patch of clear sky or uniform cloud), the photo equalizations factors are defined as follows:

$$EQPHOT_{ch} = \frac{\left(\frac{Q_{ch} + 0.5 - \phi_{ch}}{G_{ch}} \right)}{\pi \left(\frac{\phi_{ch} + 0.5 - \phi_{ch}}{G_{ch}} \right)^{1/6}}$$

where

\emptyset_{ch} = the channel offset

G_{ch} = channel gain (relative to 2100 feet, tape 5)

Q_{ch} = average multiplexer output level for the reference scene

$EQPHOT_{ch}$ = the photo equalization factor.

The photo equalizations factors may be thought of as the factors by which the apparent gains as measured by the gray wedge program must be modified in order to yield the true channel-to-channel gains and, therefore, stripe free pictures. If the calibration system shading is stable, the photo equalization factors are constant regardless of any changes in individual sensor gains. Therefore, the photo equalizations factor stability provide a measure of the shading stability of the calibration system. Because of the manner in which the gray wedge nominal values were derived, the photo equalizations factors are in this case equal to the relative channel-to-channel gains of the scanner which existed at 2100 feet in tape 5 (Kingsbury Grade, Lake Tahoe). The photo equalization factors are independent of the magnitude of the channel-to-channel shading which existed at 2100 feet in tape 5.

In theory, the photo equalization factors could be determined once and used for the entire series of tapes. Data reduction for each tape would involve only computing gain change and offset change from the gray wedge. Actually, the photo equalization factors were redetermined for all tapes where a change of location or temperature might have affected the calibration system. Therefore, in most tapes video correction is really obtained from scene data rather than the calibration system. The resulting picture quality is excellent. Only two pictures showed any striping at high light levels. One made from tape 5 was found to have been made with video correction data containing a typographic error. This introduced a 12 percent gain error in a band 2 channel and the result was a badly striped picture. When the video correction data was corrected and the picture rerun, no striping was visible. The other picture made at 8500 feet tape 12 (Yosemite) showed light (estimated 5 percent) striping in band 4 at high light levels. A recheck of the computer data used for photo equalization showed that an unidentifiable data set had been used by accident and that it differed by +4 percent in channel 19 and -3 percent in channel 21 from the average value for all tapes. The errors in other bands were of the 1 percent typical, 2 percent maximum category and apparently did not produce visible striping. The picture was not re-run.

4.8 STABILITY OF CALIBRATION SYSTEM

The photo equalizations factors derived from eleven scenes ranging from the Panamint Valley to Yosemite were studied to determine the

stability of the calibration system. Generally, for any given channel the peak deviation from the average value was in the order of 1.8 percent in band 1, 2.8 percent in band 2, 1.5 percent in band 3, and 2.6 percent in band 4. The estimated precision of the measurements is ± 5 percent.

The largest errors are found in tape 12, when the truth site was the image of an out of focus 20 percent reflectance neutral gray card. If this data is discarded, the peak errors are reduced to 1.5 percent in band 1, 1.9 percent in band 2, 1.3 percent in band 3, and 1.8 percent in band 4. It is not known why the card should affect the scanner system.

The stability of the scanner across any one panorama was such that a single video correction tape was satisfactory. This was confirmed by data taken at several points along tape 5.

4.9 SUMMARY

Table 4-2 is a summary of the video correction performance.

TABLE 4-2. PICTURES VIDEO CORRECTION
EVALUATION SUMMARY

- Ground truth data, sky and water, were successfully used to calibrate scanner calibration system
- Calibration system showed an overall 0.2 percent offset error and 5 percent gain error during the picture tests
- Destriping error summary

	Band 1		Band 2*		Band 3		Band 4	
	L	D	L	D	L	D	L	D
Tahoe	O	O	O	L	O	O	O	O
San Francisco	O	L	O	M	O	O	O	O
Yosemite	O	L	O	M	O	O	L	O

O = None, L = Light, M = Medium, H = Heavy

*Band 2 has a known video correction error of 1 percent

- In extreme dark areas, all pictures showed light striping in bands 1, 2, and 3 due to quantization limitations
- Band 4 showed no striping because of higher noise content
- Variation in sensor gains, channel-to-channel from nominals*

<u>Band</u>	<u>Percent</u>
1	10
2	9
3	6
4	2

*Nominal gains determined at Kingsbury Grade

- Variation in sensor offsets, channel-to-channel from nominals was 1 percent in all bands

5. EFFECTS OF INTERFERENCE PHENOMENON ON SCENE INFORMATION

5.1 TEST SITES AND MODE

Special engineering tests were conducted at two picture sites, Lake Tahoe and Yosemite Park, to obtain qualitative data on the effect of microphonics, coherent noise, and random noise on realistic scenes. The tests were all conducted in compression/low mode, scanning the same scene with and without the interference.

5.2 MICROPHONICS AND COHERENT NOISE TEST

The microphonics and coherent noise test was performed to determine the threshold level of microphonic and coherent noise interference on realistic scenes. Coherent sinewave interference was inserted into the scanner video output at the input to the multiplexer. Several levels and frequencies were added to the video of channels 1, 7, 10, and 13 to simulate microphonics and coherent noise. The only difference between the two tests are the frequencies involved. The microphonics frequencies were 500, 1,000, and 2,000 Hz, while the coherent noise frequencies were 5 and 10 kHz. To provide an area in the scene for comparison, only 80 percent of the picture had interference added. This was accomplished by using a gated burst oscillator which was synchronized to line start. Figures 5-1 and 5-2 present the test configuration details. The insertion levels were precalibrated before the runs with the multiplexer off and the scanner on. The aperture of the scanner was covered to prevent any video level from interfering with the calibration. The picture runs were made scanning the same scene each time and took approximately 1 hour to complete. Table 5-1 gives the sequence for this test.

5.3 RANDOM NOISE TEST

The random noise test was performed to determine the level of random noise which will degrade resolution and picture quality. The test was conducted using the same technique as used for the microphonic and coherent noise test. Several levels and two bandwidths of generator noise were inserted using a GR noise generator. The actual noise bandwidth

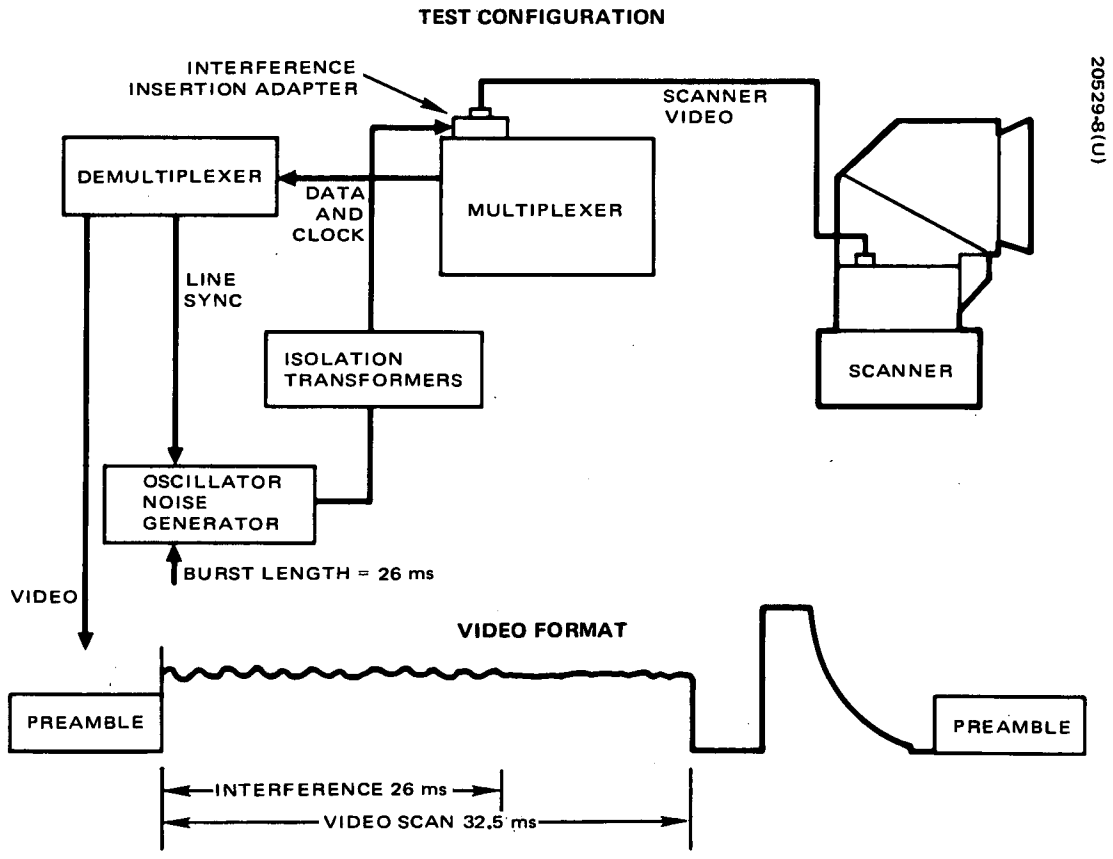


Figure 5-1. Microphonics Test

INTERFERENCE INSERTION ADAPTER

20529-9(U)

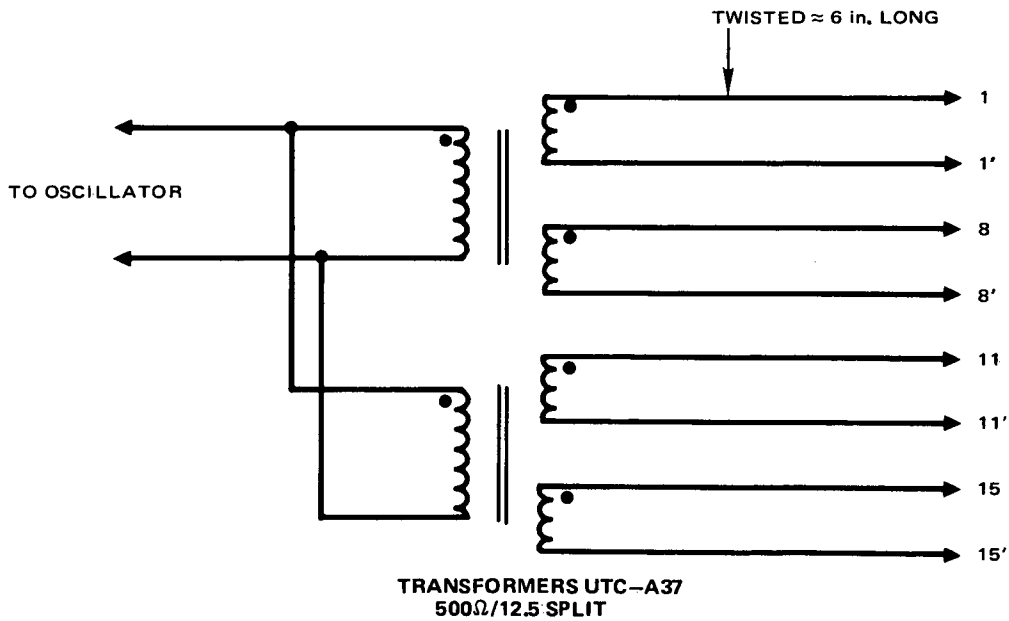
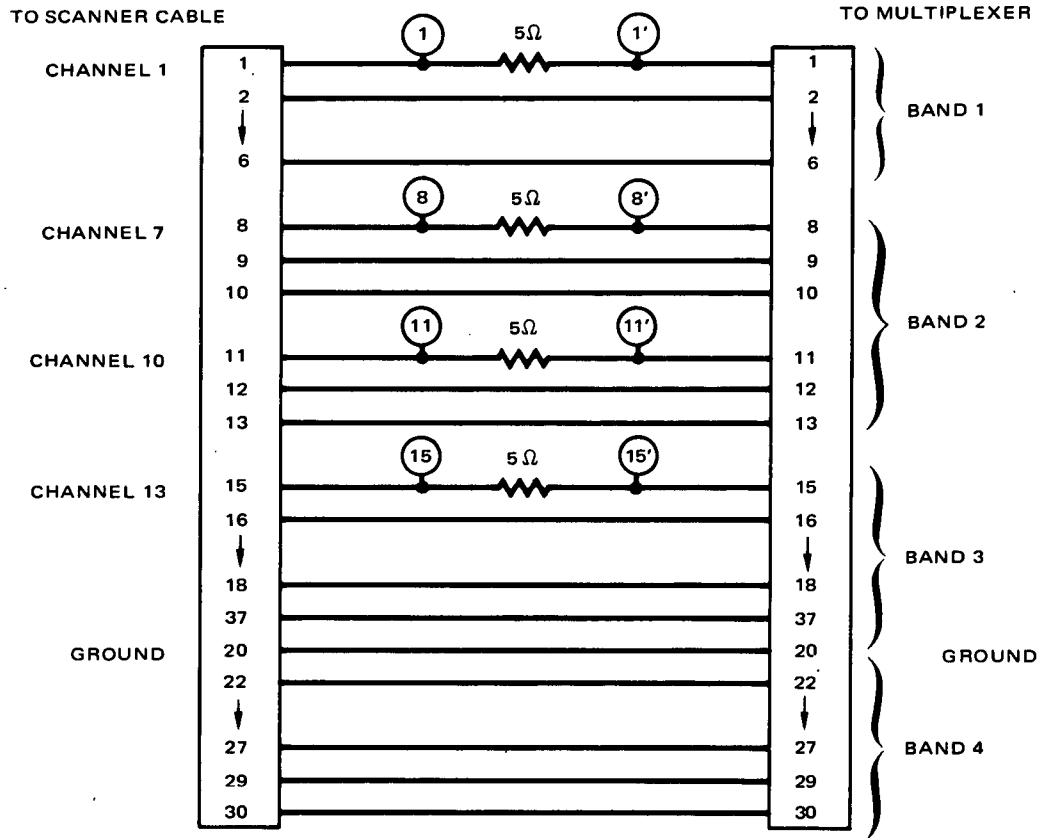


Figure 5-2. Coherent Noise Test

TABLE 5-1. TEST SEQUENCES FOR MICROPHONICS,
COHERENT NOISE, AND RANDOM NOISE

Tape	Pictures	Frequency	Levels
6	1 to 7	500 Hz	2, 4, 6, 8, 10, 12, 16 mv pp
	8 to 14	1000 Hz	2, 4, 6, 8, 10, 12, 16 mv pp
	15 to 21	2000 Hz	2, 4, 6, 8, 10, 12, 16 mv pp
11	5 to 11	5 kHz	2, 4, 6, 8, 10, 12, 16 mv pp
	12 to 17	10 kHz	2, 4, 6, 8, 10, 12 mv pp
13	4 to 6	500 kHz (BW)	1.6, 3.81, & 6.39 mv rms
	7 to 10	20 kHz (BW)	4.69, 9.7, 19.2 & 34.3 mv rms

injected into the video was determined by the bandwidth of the transformer which rolls off 3 dB at 20 kHz. The rms noise levels given below are the average of the four channel readings using an HP 3400 rms meter. Table 5-1 gives the sequence for this test.

5.4 RESULTS

With no externally induced interference, the scanner showed no evidence of microphonics or coherent noise in either the linear or compression mode pictures. However, in band 4, the low light level areas showed a slight amount of random noise due to the higher level of noise in the diode detectors.

With externally induced microphonics, the threshold level appeared to be between 10 and 16 mv, peak-to-peak. This depended on the scene brightness and content for both compression and linear mode pictures. For the range of levels used (i.e., 2 to 16 mv, peak-to-peak), no apparent threshold level was discernible for the coherent noise test. This was also the case for the random noise test, but traces of noise were discernible in flat dark areas for most of the levels used.

6. EVALUATION OF FALSE COLOR COMPOSITE IMAGES AS PRODUCED FROM MSS IMAGERY

6.1 ASSIGNMENT OF COLORS TO BANDS

False color imagery is produced from MSS/GPE pictures by assigning specific colors to three of the MSS bands and photographically superimposing these color images on paper or transparent film. The colors assigned to the bands are as follows: band 1 - blue; band 2 - green; band 3 - red. Those color assignments occur in the same order as the primary colors of the visible spectrum, but cause a shift in color from the familiar real world colors to a so-called "false color" representation. The black and white GPE negatives are treated exactly the same as separation negatives used in three-color printing. Band 4 was not generally utilized for color production, since three primary colors are customarily used for color printing and band 4 is not immediately adjacent to the visible spectrum. This does not rule out the use of four colors or other combinations of bands with three colors. For example, use may be made in operations of the combination: band 1, blue; band 2, green; band 4, red.

The false color representation of real world colors used in these tests results in the green portion of the spectrum (0.5 to 0.6 micron; band 1) being imaged as a blue color, the red portion of the spectrum (0.6 to 0.7 micron; band 2) being imaged as green, and the near infrared portion of the spectrum (0.7 to 0.8 micron; band 3) being imaged as red.

6.2 EFFECT OF COLOR ASSIGNMENTS ON SCENE OBJECTS

The real world pictures produced in false color imaged water in lakes as dark blue, due to the somewhat low reflectivity in the green (0.5 to 0.6 micron) portion of the spectrum, and negligible reflectivity in the red (0.6 to 0.7 micron) and infrared (0.7 to 0.8 micron) portions of the spectrum. Trees and plants were imaged as a bright red, due to the very high reflectivity of chlorophyll-bearing leaves in the near infrared. Rocks and granite mountains produced an essentially neutral color (similar to real world appearance) due to relatively uniform reflectivity in the 0.5 to 0.8 micron spectral region. Sky was reproduced as blue due to Rayleigh scattering in the green (0.5 to 0.6 micron) portion of the spectrum, with low scattering taking place in the 0.6 to 0.8 micron region.

The MSS false color imagery compared favorably with test photographs taken with infrared color film at the same time the scanner images were being recorded. The photographic tests utilized color film which is sensitized to operate within the 0.5 to 0.8 micron region of the spectrum. The film is actually sensitized to the blue end of the spectrum, but a filter is used over the camera lens to absorb radiation below 0.5 micron. The film chemistry is programmed to print blue for radiation from 0.5 to 0.6 micron, green for radiation from 0.6 to 0.7 micron, and red for radiation from 0.7 to 0.8 micron. The film is therefore programmed in a similar way to the color assignments made to the MSS bands 1, 2, and 3 images.

The MSS imagery displayed similar color qualities to the photographic imagery; i.e., red trees, blue sky, dark blue water, etc., except that the MSS rendering of rocks and granite was superior to the photographic reproduction. The MSS reproduced granite mountains as a relatively neutral (gray) color, but the color film showed a decided shift to the blue for all mountain images. This is caused by a relative change in sensitivity of the emulsion layers of the color film, which is usually caused by heat and age. Film not exposed to heat and which is absolutely fresh should not show any color shift of neutral colored objects toward the blue. The MSS imagery is not subject to the heat sensitivity that degrades color film, and so false color reproduction with the MSS should be predictable and repeatable, as long as GPE film density and contrast are controlled.

6.3 COLOR PROCESSING PROBLEMS

A major problem encountered in the false color production with the GPE films was the inconsistencies in contrast and overall density. The density range intended for the negatives used in color production is from 0.30 to 1.95. However, the actual densities deviated from this by as much as 0.20 at the high end of the scale. There were also general density gradients across the original frames by the same amount. Variations of brightness between the two crater lamps also accounted for a portion of the density variations. The density and contrast variations made color printing difficult because of difficulties of achieving uniform color balance.

6.4 FILM DYES

The color of the dyes used in producing the false color pictures from MSS films are actually the complimentary colors of blue, green and red, namely, yellow, magenta (reddish), and cyan (bluish). Those colors are used because the color mixing that takes place in a color transparency or color print is a subtractive process that results in a positive color image. If three projectors are used, however, to reconstruct a false color picture on a white screen, black and white positives of each band are projected

simultaneously on the screen with the corresponding blue, green, or red filter placed over the lens of the appropriate projector. The images are made to register and a false color picture is created. With the projection method, the color mixing that takes place is additive; hence, the use of the blue, green, and red filters.

7. REFLECTANCE TESTS

7.1 MEASUREMENTS OF SCANNER

On 24 February 1972, a number of growing plants and a few reflectance sample cards were presented to the engineering model scanner, with sun lighting, and the output voltages were measured. These are listed in Table 7-1. The scanner view was vertically down and the samples were horizontal and 6 feet below the scanner. A visually black cloth, specimen No. 4, was draped to reduce spectral reflections from the scanner support. Figure 7-1 shows the plants from the same aspect as viewed by the scanner with the same illumination angle. The square arrays shown are approximately 18 inches on a side. The plants were nursery seedlings, except for the broccoli and lettuce, which were mature, and had been transplanted to provide a tighter grouping.

The 80 and 20 percent cards are from the Munsell Color Co., and the 1.0 card was provided by W. A. Hovis of GSFC. Cards had been prepared with black and white stripes proportioned to give different average values of reflectance for each card, but it was found that moving such a card to and fro in a direction perpendicular to the stripes caused a signal variation of 15 percent, since the stripes enter different parts of the aperture. The cards for which data are tabulated were uniform over the surfaces.

The Brussels sprouts were shifted laterally a few inches while observing the maximum variation in signal. This variation was 20 percent for bands 1 and 2, 10 percent for band 3, and 12 percent for band 4.

The data shows that rotating the plants through 180 degrees reduced the signal. This may be due to the same effect as the Brussels sprouts and striped-cards variation; that is, a change in the ratio of light to dark area entering the aperture. However, as the change was always a decrease, it may indicate that in the initial orientation the leaves had turned toward the sun, increasing their apparent reflectance.

Specimen No. 3 was a black velveteen cloth shaded from the sunlight to furnish a dark scene.

The readings on the lettuce sample are thought to be increased for the reason that the rather large box had to be tilted toward the sun to be beneath the scanner, because of interference with the scanner support.

TABLE 7-1. SBRC PATIO MEASURED VOLTS

No.	Description	Band			
		1	2	3	4
1	80 percent reflectance	4.40	4.50	4.00	4.40
3	20 percent reflectance	1.30	1.35	1.30	1.15
3	Shadowed black velveteen	0.00	0.00	0.05	0.15
4	'Black' cloth	0.20	0.25	1.40	2.20
5	1.0 reflectance	5.00	5.40	4.60	4.80
6	Bell pepper	0.44	0.36	2.50	2.90
7	Grass, blue fescue	0.39	0.34	2.25	2.90
8	Strawberry, tioga	0.30	0.29	2.70	3.40
9	Strawberry, 180 degrees	0.24	0.22	2.20	2.80
10	Strawberry, 0 degree repeat	0.30	0.30	2.70	3.40
11	Brussels sprouts	0.31	0.30	2.10	2.50
12	Brussels sprouts, 180 degrees	0.30	0.30	2.00	2.40
13	Brussels sprouts, 0 degree repeat	0.30	0.28	2.20	2.50
14	Tomato	0.44	0.35	2.50	3.00
15	Tomato, 180 degrees	0.40	0.34	2.40	2.90
16	Dichondra	0.29	0.24	2.30	2.90
17	Broccoli	0.41	0.39	2.35	2.80
18	Broccoli, 3 inch movement	0.40	0.39	2.10	2.50
19	Sand, dry	1.35	1.75	2.00	2.00
20	Sand, wet	0.62	0.84	1.00	1.00
21	Red pumice	0.18	0.50	0.72	0.80
22	Lettuce	0.58	0.48	2.80	3.40
23	Dirt, damp	0.19	0.30	0.49	0.59
24	Dirt, wet	0.17	0.24	0.38	0.50



a) BELL PEPPER



b) GRASS, BLUE FESCUE



c) STRAWBERRY, TIOGA



d) BRUSSEL SPROUTS



e) TOMATO



f) DICHONDRA



g) BROCCOLI



h) LETTUCE

Figure 7-1. Plants as Viewed by MSS

7.2 MEASUREMENTS OF SUN

The solar spectral irradiance through the atmosphere was measured at the same time as the scanner measurements by GFSC personnel with equipment which had been used in a program of airborne solar measurements*. Further information on the instruments can be found in the referenced article. The particular instruments, and the experimenter who operated them at SBRC were the following:

- 1) Perkin-Elmer monochromator, M. P. Thekaekara, A. Winker.
- 2) Angstrom pyrhelimeter 7635, C. H. Duncan.
- 3) Leiss monochromator, S. Parke.

Solar irradiance measurements were also made by W. A. Hovis. The data was reduced by the experimenters and has been furnished for use in scanner data reduction.

7.3 APPARENT REFLECTANCE CALCULATION

On 3 May 1972 the engineering model scanner sensitivities were measured with reference to the GSFC integrating sphere. These data were combined with the measurements discussed above, using the equations shown in subsection 7.6, to calculate the apparent perfectly diffuse reflectance corresponding to each voltage. Zero radiance readings were assumed to be zero volt, except for 0.05 volt in band 4, the value measured at the May recalibration. This assumption also implies some radiant signal from the shadowed black velveteen in the reflectance test. The results are listed in Table 7-2.

The band 4 reflectance values are obviously high. One possible reason investigated was the spectral distribution of sun compared to the integrating sphere. From Equation 3, 4.0 volts should be the signal for

$$(N_{sb}) (R_{pk}) \int_0^{\infty} R(\lambda) N_{sph}(\lambda) d\lambda / \int_{bl}^{bu} N_{sph}(\lambda) d\lambda$$

were the sun used as the standard, this could be expressed as

$$(N_{sb}) (R_{pk}) \int_0^{\infty} R(\lambda) H_{\odot\odot}(\lambda) d\lambda / \int_{bl}^{bu} H_{\odot\odot}(\lambda) d\lambda$$

*Thekaekara, Kruger and Duncan, Appl. Opt. 8, 1713 (1969).

TABLE 7-2. CALCULATED REFLECTANCE

No.	Description	Band				Band 4 Corrected
		1	2	3	4	
1	80 percent reflectance	0.709	0.830	0.801	1.183	0.86
2	20 percent reflectance	0.210	0.249	0.261	0.300	0.22
3	Shadowed black velveteen	0.000	0.000	0.010	0.027	0.02
4	'Black' cloth	0.032	0.046	0.283	0.591	0.43
5	1.0 reflectance	0.817	1.011	0.936	1.313	0.95
6	Bell pepper	0.072	0.067	0.511	0.792	0.57
7	Grass, blue fescue	0.064	0.064	0.465	0.803	0.58
8	Strawberry, tioga	0.050	0.055	0.563	0.952	0.69
9	Strawberry, 180 degrees	0.040	0.042	0.465	0.793	0.57
10	Strawberry, 0 degree repeat	0.050	0.058	0.573	0.971	0.70
11	Brussels sprouts	0.053	0.058	0.449	0.717	0.52
12	Brussels sprouts, 180 degrees	0.051	0.059	0.429	0.690	0.50
13	Brussels sprouts, 0 degree repeat	0.051	0.055	0.477	0.728	0.53
14	Tomato	0.077	0.071	0.553	0.896	0.65
15	Tomato, 180 degrees	0.070	0.069	0.533	0.869	0.63
16	Dichondra	0.051	0.049	0.515	0.877	0.63
17	Broccoli	0.074	0.081	0.535	0.862	0.62
18	Broccoli, 3 inch movement	0.072	0.081	0.481	0.773	0.56
19	Sand, dry	0.247	0.370	0.463	0.623	0.45
20	Sand, wet	0.114	0.178	0.233	0.305	0.22
21	Red pumice	0.033	0.107	0.169	0.244	0.18
22	Lettuce	0.109	0.104	0.668	1.106	0.80
23	Dirt, damp	0.036	0.066	0.119	0.182	0.13
24	Dirt, wet	0.032	0.053	0.093	0.154	0.11

The latter expression was found to be 3.5 percent greater than the former for band 4, too small an amount to account for the high reflectance values calculated.

Another possibility is that the samples observed by the MSS were irradiated more strongly than the sun and sky measurements indicate. The source of added irradiance could be the "black" background cloth beneath the samples, which was also draped upon the scanner supports, which supports had some specular reflections. The background cloth was reflective in band 4, as indicated in the data. As a test of this possibility, we assign 95 percent diffuse reflectance to the 1.0 test card and reduce the calculated values of the other samples in the same proportion, with the results also shown in Table 7-2, as band 4 corrected. This procedure gives reflectances which agree more closely with expectations.

The reflectances shown for the two Munsell cards may be compared with calibration measurements of reflectance (performed in 1969), averaged over each band, which were

<u>Card</u>	<u>Band 1</u>	<u>Band 2</u>	<u>Band 3</u>	<u>Band 4*</u>
80 percent	0.775	0.79	0.795	0.78
20 percent	0.240	0.238	0.225	0.20

*Band 4 values are approximate, as the data ends at 1.0 micron.

7.4 PREDICTED SIGNALS

If further atmospheric attenuation is applied and a sky contribution added, the signal voltage which would have been produced by the scanner in orbit can be calculated by equations shown in subsection 7.6. This has been done, along with allowance for the effect of differing sun zenith angle, and the results appear in Table 7-3 for two sun zenith angles. Note that the listing is regrouped from the previous tables. Signals will limit at 4.0 volts in the transmitting chain used in orbit.

The atmospheric transmission data from the Table Mountain test was used to predict the orbital signals from the same materials, if at such a location, and these are listed in Table 7-4. The notation "SKY X 0.5" indicates that sky radiance was arbitrarily multiplied by this factor to translate from SBRC measurements to a rough estimate for Table Mountain.

7.5 CONCLUSIONS

The patterns of dark and light in the plants and on some sample cards, having dimensions near enough to telescope aperture dimensions, influence the observed signal level substantially, depending upon position.

TABLE 7-3. CALCULATED SIGNAL VOLTAGE
IN SPACE FOR TWO ZENITH ANGLES

SBRC Patio Zenith Angle = 30.0 EXT COEF 0.2245 0.1790 0.1702 0.2022 SKY X 1.0					
No.	Description	Band			
		1	2	3	4
5	1.0 reflectance	5.452	6.517	5.560	3.947
2	20 percent reflectance	1.865	1.901	1.716	0.943
1	80 percent reflectance	4.814	5.420	4.791	3.561
6	Bell pepper	1.049	0.799	3.139	2.402
7	Grass, blue fescue	1.002	0.780	2.877	2.434
8	Strawberry, tioga	0.919	0.726	3.436	2.876
11	Brussels sprouts	0.937	0.744	2.786	2.179
14	Tomato	1.079	0.823	3.379	2.710
16	Dichondra	0.925	0.690	3.162	2.654
17	Broccoli	1.061	0.883	3.276	2.609
22	Lettuce	1.268	1.023	4.034	3.333
19	Sand, dry	2.083	2.634	2.866	1.901
20	Sand, wet	1.297	1.471	1.556	0.958
23	Dirt, damp	0.836	0.793	0.907	0.593
24	Dirt, wet	0.813	0.714	0.759	0.510
21	Red pumice	0.819	1.041	1.192	0.777
SBRC Patio Zenith Angle = 55.0 EXT COEF 0.2245 0.1790 0.1702 0.2022 SKY X 1.0					
No.	Description	Band			
		1	2	3	4
5	1.0 reflectance	3.767	4.312	3.568	2.377
2	20 percent reflectance	1.432	1.358	1.160	0.584
1	80 percent reflectance	3.352	3.610	3.087	2.147
6	Bell pepper	0.901	0.652	2.052	1.455
7	Grass, blue fescue	0.870	0.641	1.888	1.474
8	Strawberry, tioga	0.816	0.606	2.238	1.738
11	Brussels sprouts	0.828	0.618	1.831	1.322
14	Tomato	0.920	0.668	2.202	1.639
16	Dichondra	0.820	0.583	2.066	1.605
17	Broccoli	0.908	0.707	2.138	1.579
22	Lettuce	1.043	0.796	2.612	2.011
19	Sand, dry	1.574	1.827	1.881	1.156
20	Sand, wet	1.062	1.083	1.060	0.593
23	Dirt, damp	0.762	0.649	0.654	0.375
24	Dirt, wet	0.747	0.598	0.561	0.326
21	Red pumice	0.751	0.807	0.832	0.485

TABLE 7-4. CALCULATED SIGNAL VOLTAGE IN SPACE
FOR TWO ZENITH ANGLES, TABLE
MOUNTAIN CONDITIONS

Table MTN Zenith Angle = 30.0 EXT COEF 0.1461 0.0908 0.0569 0.0707 SKY X 0.5					
No.	Description	Band			
		1	2	3	4
5	1.0 reflectance	5.504	7.161	6.659	5.132
2	20 percent reflectance	1.646	1.912	1.939	1.193
1	80 percent reflectance	4.818	5.914	5.715	4.626
6	Bell pepper	0.769	0.658	3.688	3.106
7	Grass, blue fescue	0.718	0.637	3.366	3.149
8	Strawberry, tioga	0.629	0.575	4.051	3.728
11	Brussels sprouts	0.648	0.596	3.254	2.814
14	Tomato	0.801	0.685	3.981	3.510
16	Dichondra	0.636	0.534	3.715	3.436
17	Broccoli	0.782	0.754	3.855	3.378
22	Lettuce	1.004	0.913	4.785	4.327
19	Sand, dry	1.881	2.745	3.352	2.449
20	Sand, wet	1.036	1.422	1.744	1.212
23	Dirt, damp	0.540	0.651	0.946	0.734
24	Dirt, wet	0.515	0.561	0.765	0.625
21	Red pumice	0.521	0.933	1.296	0.975
Table MTN Zenith Angle = 55.0 EXT COEF 0.1461 0.0908 0.0569 0.0707 SKY X 0.5					
No.	Description	Band			
		1	2	3	4
5	1.0 reflectance	3.640	4.704	4.379	3.287
2	20 percent reflectance	1.167	1.306	1.304	0.771
1	80 percent reflectance	3.200	3.897	3.764	2.964
6	Bell pepper	0.605	0.495	2.443	1.993
7	Grass, blue fescue	0.572	0.481	2.233	2.021
8	Strawberry, tioga	0.515	0.441	2.680	2.391
11	Brussels sprouts	0.528	0.455	2.160	1.807
14	Tomato	0.625	0.513	2.634	2.252
16	Dichondra	0.519	0.415	2.461	2.204
17	Broccoli	0.613	0.557	2.552	2.167
22	Lettuce	0.756	0.660	3.158	2.773
19	Sand, dry	1.318	1.846	2.224	1.574
20	Sand, wet	0.776	0.990	1.176	0.784
23	Dirt, damp	0.458	0.490	0.657	0.478
24	Dirt, wet	0.442	0.432	0.538	0.409
21	Red pumice	0.446	0.673	0.884	0.632

The calculated reflectances were anomalously high for band 4, possibly due to added irradiance from a background reflection onto the samples.

If the reflectances are decreased to allow for the above anomaly, the predicted signals to be obtained in orbit appear to be of reasonable size. Some signals show limiting, but plants in the natural scene will not often be crowded together as in the samples used.

7.6 DERIVATION OF SCANNER RESPONSE

The response of a channel of the scanner to a scene may be represented as an output voltage per input spectral radiance, with units of $V/(mW \cdot cm^{-2} \cdot ster^{-1})$, which may be made up of two factors, R_{pk} , the value at the maximum, and $R(\lambda)$, the value at any wavelength relative to the maximum. The scanner signal voltage from a scene of spectral radiance $N(\lambda)$ would be

$$S = R_{pk} \int R(\lambda) N(\lambda) d\lambda \quad (1)$$

The scanner is calibrated by exposing it to the GSFC integrating sphere, and requiring an output of 4.0 volts when the sphere radiance is a specified value, N_{sb} , between band edge wavelengths, where the subscript b indicates the band number. The value of spectral radiance of the fully powered sphere $N_{sph}(\lambda)$, is provided by GSFC. The full-power sphere radiance between band limits is

$$N_b = \int_{bl}^{bu} N_{sph}(\lambda) d\lambda \quad (2)$$

where bl and bu are the band lower and upper limits

Then, for the calibrated condition,

$$4.0 \text{ volts} = \frac{N_{sb}}{N_b} R_{pk} \int_0^{\infty} R(\lambda) N_{sph}(\lambda) d\lambda \quad (3)$$

which may be solved for R_{pk} :

$$R_{pk} = \frac{4.0 \text{ volts} \int_{bl}^{bu} N_{sph}(\lambda) d\lambda}{N_{sb} \int_0^{\infty} R(\lambda) N_{sph}(\lambda) d\lambda} \quad (4)$$

The radiance of the various samples observed in the tests at Santa Barbara were the result of reflection of sun and sky irradiance. The sun's spectrum for a zenith angle Z such that $\sec Z = 1.5$ was furnished as irradiance on a surface normal to the sun's rays. The sky data was given as spectral irradiance on a horizontal surface, considered constant during the measurements.

From the standard sun spectral irradiance outside the atmosphere, band average values of the extinction coefficient can be obtained, as follows:

$$e^{-K(1.5)} = \frac{\int R(\lambda) H_{\odot}(\lambda) d\lambda}{\int R(\lambda) H_{\odot o}(\lambda) d\lambda} \quad (5)$$

where

K = extinction coefficient
 $H_{\odot}(\lambda)$ = solar spectral irradiance

Subscript o indicates outside the atmosphere. Several values from the above calculations are shown in Table 7-5.

Then the spectral radiance of a sample would be, assuming perfectly diffuse reflectance,

$$N(\lambda) = \frac{\rho}{\pi} (H_{\odot o}(\lambda) e^{-K \sec Z} \cos Z + H_{sk}(\lambda)) \quad (6)$$

TABLE 7-5. PERTINENT CALCULATED VALUES

Band	Specified Radiance, N_{sb}^*	Sphere Radiance, N_b^*	Effective Sphere Radiance, $R(\lambda)N_{sph}(\lambda) d\lambda^*$	Peak Sensitivity, $R_{pk} V/$ *	Extinction Coefficient
1	2.48	2.08	2.02	1.657	0.225
2	2.00	3.73	3.73	2.000	0.179
3	1.76	5.12	5.62	2.069	0.170
4	4.60	17.97	11.25	1.389	0.202

*Radiance units are $mW \cdot cm^{-2} \cdot ster^{-1}$

where

$$\begin{aligned} \rho &= \text{reflectance} \\ H_{sk}(\lambda) &= \text{sky irradiance} \end{aligned}$$

Thus the signal would be, substituting in Equation 1,

$$S = \frac{R_{pk} \rho}{\pi} [e^{-K \sec Z} \cos Z \int R(\lambda) H_{\odot\odot}(\lambda) d\lambda + \int R(\lambda) H_{sk}(\lambda) d\lambda] \quad (7)$$

Equation 7 was solved for apparent reflectance for the various data sets using typical $R(\lambda)$ shapes, with results as shown in Table 7-2.

Had these samples been viewed from space (and been large enough to fill the field of view) the radiance would have been attenuated by the zenith-path atmosphere, e^{-K} , and augmented by the sky radiance, which is

$$N_{sk} = \frac{k_s}{\pi} \int R(\lambda) H_{sk}(\lambda) d\lambda \quad (8)$$

where k_s = a factor accounting for non-uniform distribution = 0.5 arbitrary, then the scanner signal in space would be

$$S' = S e^{-K} + R_{pk} N_{sk} \quad (9)$$

Elements of Equation 9 are shown in Table 7-6.

TABLE 7-6. EQUATION 9 CONTRIBUTIONS

Band	Zenith Attenuation	Sky Signal, Volts
1	0.799	0.6
2	0.836	0.4
3	0.844	0.2
4	0.816	0.0

APPENDIX A. PICTURE SITES

A. 1 SITE REQUIREMENTS

The requirements established for good picture taking sites were as follows:

- 1) A scene greater than 5 miles away
- 2) Visibility greater than 30 miles with little or no haze
- 3) No foreground contamination
- 4) A large field of view
- 5) Level parking areas,
- 6) A variety of terrain, such as rocks, mountains, vegetation, snow, water, buildings, etc.

A. 2 SELECTED SITES

The sites selected are given in Table A-1. The sites are numbered so they can be identified in Figures A-1 through A-7, which are maps which display the scenes viewed.

A. 3 TEST OPERATIONS SUMMARY

The test operating conditions are summarized as follows:

- 1) Temperature range: 30 to 80° F
- 2) Humidity: 5 to 80 percent
- 3) Vibration: 1200 miles in non-air ride truck
- 4) Altitude: 100 to 8100 feet

TABLE A-1. PANORAMIC PICTURE SITES

Lone Pine Area (Figure A-1)

1. View from Lone Pine Station Road 2 miles east of Lone Pine, scanning from 190 to 300 degrees.
2. View from Long John Canon Road 5 miles east of Lone Pine, scanning from 195 to 290 degrees.

Panamint Valley Area (Figure A-2)

3. View from Padre Crowley Point Monument, scanning from 95 to 190 degrees.

Lake Tahoe Area (Figures A-3 and A-4)

4. View of Carson Valley from Route 50, 4 miles west of Route 395, scanning from 110 to 190 degrees toward Minden, Nevada.
5. View of west shore of Lake Tahoe from Kingsbury Hill, scanning from 225 to 310 degrees.
6. View of south and east shore of Lake Tahoe from Meeks Bay, scanning from 45 to 150 degrees.

San Francisco Area (Figure A-5)

7. View of San Francisco City area from the north end of the Golden Gate Bridge Vista Point, scanning from 70 to 210 degrees.
8. View of San Francisco from Berkeley Hills, Lawrence Science Center parking lot, scanning from 170 to 300 degrees.
9. View of San Francisco from Twin Peaks, scanning from 10 to 110 degrees.

Table A-1 (continued)

Yosemite National Park Area (Figure A-6)

10. View of Yosemite Valley from Wawona tunnel, scanning from 45 to 100 degrees.
11. View of Half Dome and Cathedral Mountain Range from Glacier Point, scanning from 15 to 155 degrees.

Santa Barbara Area (Figure A-7)

12. View of Santa Barbara City from KEY-TV transmitter site, scanning from 350 to 80 degrees.

A. 4 GENERAL OBSERVATIONS

During the 8 days of picture taking, no equipment problems were incurred. However, it was observed that the scan monitor pulse decreased in amplitude at cold temperature in the range of 32 to 35° F. It was found that twisting the casting counterclockwise or increasing the power supply from -24.5 to -27.5 volts restored the normal level. Furthermore, a noticeable increase in scanner vibration level was noted at these same low temperatures.

A. 5 TAPE INVENTORY

A complete inventory of all tape footage recorded during the picture taking test is given in Table A-2. The table gives the tape number, footage, location, mode, and date.

A. 6 PICTURE EQUIPMENT CONFIGURATION

Figure A-8 is a block diagram of the equipment configuration used to take the pictures. Figure A-9 is a photograph showing the scanner and rotab mounted in the truck. Although the truck was jacked up to reduce vibration, it still vibrated slightly in heavy winds. Therefore, in areas where terrain and weather conditions permitted, the scanner and rotab were set up outside on the ground as shown in Figure A-10.

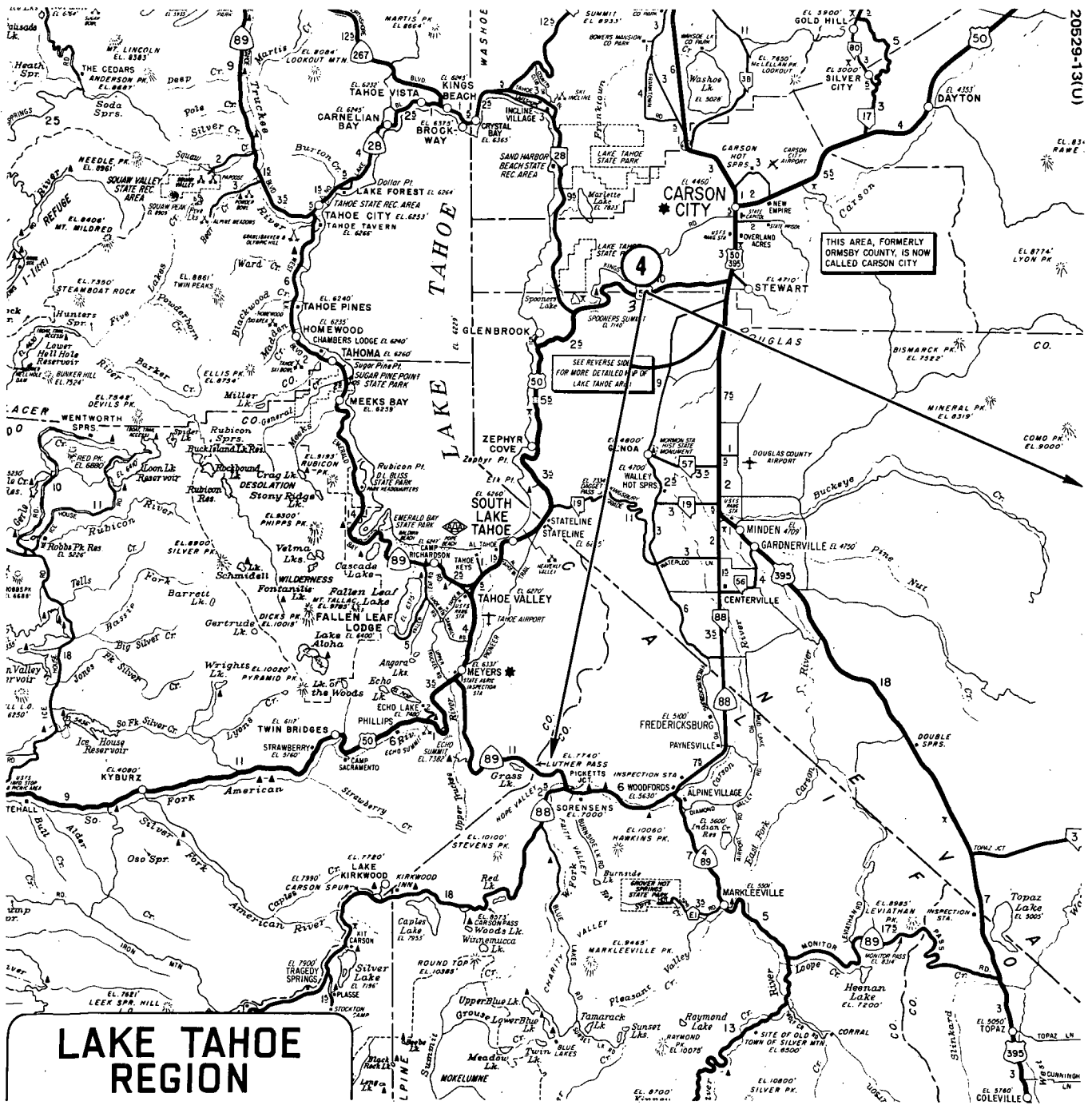


Figure A-3. Lake Tahoe Area - Carson Valley Region

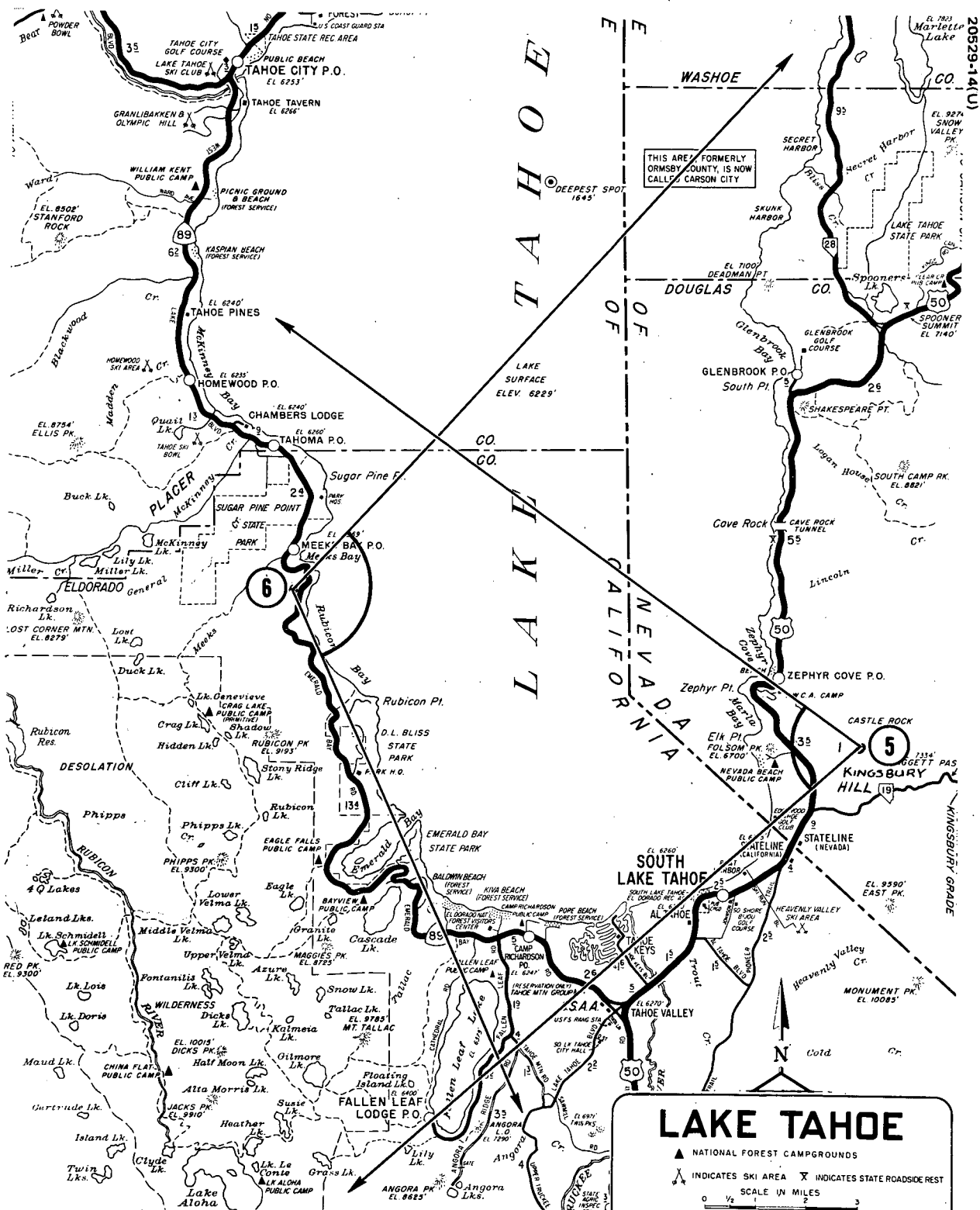


Figure A-4. Lake Tahoe Area - Lake Region

TABLE A-2. PANORAMIC PICTURES TAPE INVENTORY

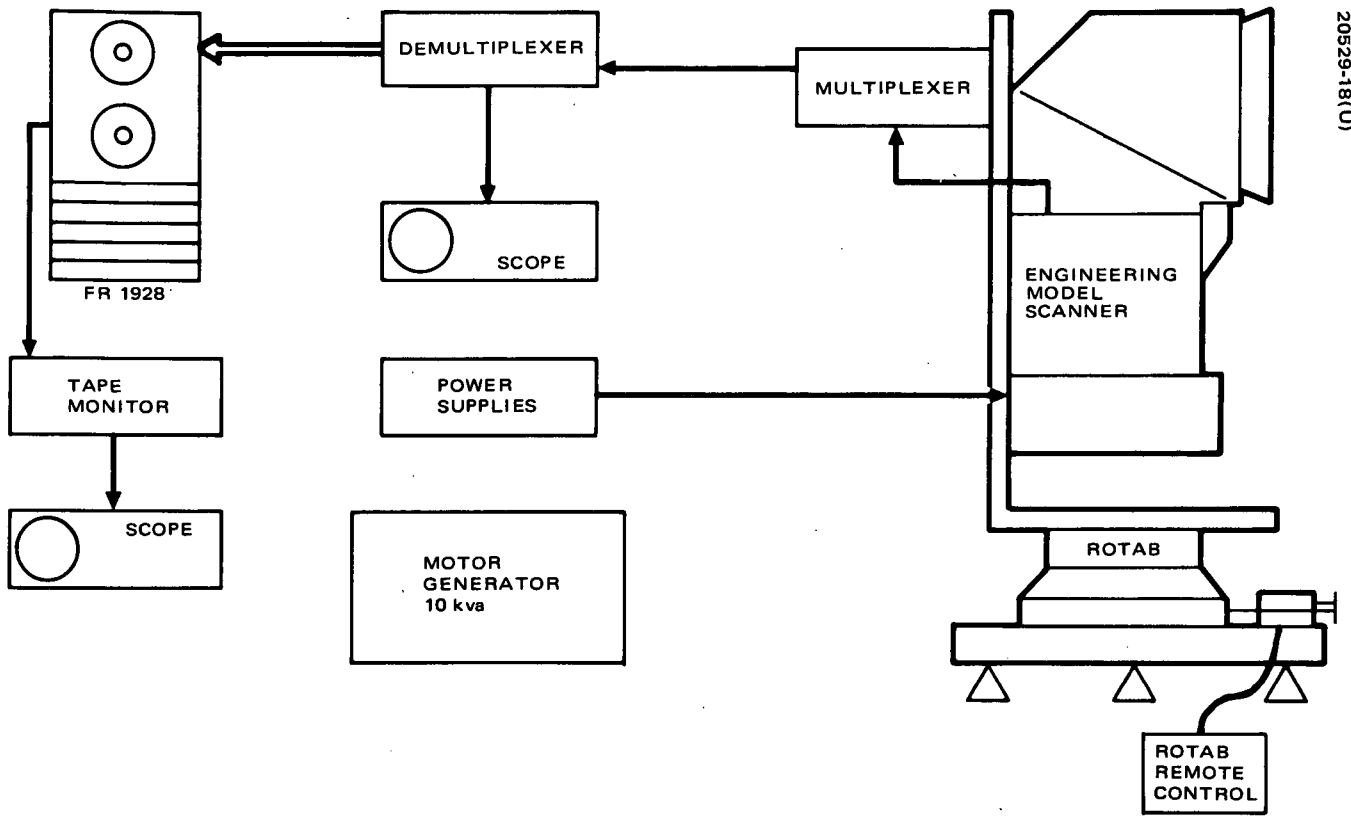
Date	Location	Footage	Tape No.
5/19/72	<u>Lone Pine from Lone Pine Station Road</u>		1
	<ol style="list-style-type: none"> 1. Calibration Seq 1 400' per Band 2. PIX <ol style="list-style-type: none"> 1. Linear/Low Filter Out 2. Comp/Low Filter Out 3. Linear/Low Filter In 4. Comp/Low Filter In 5. (Rotab Stopped) Comp/Low Filter Out 	100-2100 2200-2900 3000-3700 3750-4450 4500-5200 5250-5650	
5/19/72	<u>Panamint Valley from Padre Crowley Point</u>		2
	<ol style="list-style-type: none"> 1. Calibration Seq 2 Flat Field 2. PIX <ol style="list-style-type: none"> 1. Linear/Low Filter Out 2. Comp/Low Filter Out 3. Linear/Low Filter In 4. Comp/Low Filter In 5. Comp/High Filter In 	100-500 600-2100 2200-3500 3600-5038 5100-6500 6600-8000	
5/20/72	<u>Lone Pine from Long John Canon Road</u>		3
	<ol style="list-style-type: none"> 1. Calibration Seq 1 2. PIX <ol style="list-style-type: none"> 1. Linear/Low Filter Out 2. Comp/Low Filter Out 3. Linear/Low Filter In 4. Comp/Low Filter In 	100-1950 2100-3400 3500-4800 4900-6300 6400-7800	
5/21/72 4:30 pm	<u>Carson, Nevada from Vista Point on Rt 50</u>		4
	<ol style="list-style-type: none"> 1. Calibration Seq 1 2. PIX <ol style="list-style-type: none"> 1. Linear/Low Filter Out 2. Comp/Low Filter Out 3. Linear/Low Filter In 4. Comp/Low Filter In 5. Rotab Stopped Filter In 	100-1900 2000-2989 3100-4120 4200-5200 5300-6320 6400-6800	
5/22/72 11:00 am	<u>Kingsbury Grade, South Lake Tahoe</u>		5
	<ol style="list-style-type: none"> 1. Calibration Seq 1 2. PIX <ol style="list-style-type: none"> 1. Linear/Low Filter Out 2. Comp/Low Filter Out 3. Linear/Low Filter In 4. Comp/Low Filter In 3. Rerun <ol style="list-style-type: none"> 1. Linear/Low Filter Out 2. Comp/Low Filter Out 3. Comp/High Filter In 	100-1950 2100-3050 3100-4035 4100-5030 5100-5990 6050-6920 7000-7850 7900-8800	

Table A-2 (continued)

Date	Location	Footage	Tape No.																																																																																								
5/22/72 12:15 pm	<p><u>Kingsbury Grade, South Lake Tahoe</u></p> <p>1. Microphonics Test - Comp/Low - 26 Millisec Burst</p> <table data-bbox="362 436 1204 953"> <thead> <tr> <th></th> <th><u>Freq</u></th> <th><u>Level</u></th> <th></th> </tr> </thead> <tbody> <tr> <td>2. PIX</td> <td>1. 500 Hz</td> <td>2 mvpp</td> <td>100-500</td> </tr> <tr> <td></td> <td>2. 500 Hz</td> <td>4 mvpp</td> <td>550-950</td> </tr> <tr> <td></td> <td>3. 500 Hz</td> <td>6 mvpp</td> <td>1000-1400</td> </tr> <tr> <td></td> <td>4. 500 Hz</td> <td>8 mvpp</td> <td>1450-1850</td> </tr> <tr> <td></td> <td>5. 500 Hz</td> <td>10 mvpp</td> <td>1900-2300</td> </tr> <tr> <td></td> <td>6. 500 Hz</td> <td>12 mvpp</td> <td>2350-2750</td> </tr> <tr> <td></td> <td>7. 500 Hz</td> <td>16 mvpp</td> <td>2800-3200</td> </tr> <tr> <td></td> <td>8. 1000 Hz</td> <td>2 mvpp</td> <td>3250-3650</td> </tr> <tr> <td></td> <td>9. 1000 Hz</td> <td>4 mvpp</td> <td>3700-4100</td> </tr> <tr> <td></td> <td>10. 1000 Hz</td> <td>6 mvpp</td> <td>4150-4550</td> </tr> <tr> <td></td> <td>11. 1000 Hz</td> <td>8 mvpp</td> <td>4600-5000</td> </tr> <tr> <td></td> <td>12. 1000 Hz</td> <td>10 mvpp</td> <td>5050-5450</td> </tr> <tr> <td></td> <td>13. 1000 Hz</td> <td>12 mvpp</td> <td>5500-5900</td> </tr> <tr> <td></td> <td>14. 1000 Hz</td> <td>16 mvpp</td> <td>5950-6350</td> </tr> <tr> <td></td> <td>15. 2000 Hz</td> <td>2 mvpp</td> <td>6400-6800</td> </tr> <tr> <td></td> <td>16. 2000 Hz</td> <td>4 mvpp</td> <td>6850-7250</td> </tr> <tr> <td></td> <td>17. 2000 Hz</td> <td>6 mvpp</td> <td>7300-7700</td> </tr> <tr> <td></td> <td>18. 2000 Hz</td> <td>8 mvpp</td> <td>7750-8050</td> </tr> <tr> <td></td> <td>19. 2000 Hz</td> <td>10 mvpp</td> <td>8100-8400</td> </tr> <tr> <td></td> <td>20. 2000 Hz</td> <td>12 mvpp</td> <td>8450-8750</td> </tr> <tr> <td></td> <td>21. 2000 Hz</td> <td>16 mvpp</td> <td>8800-9100</td> </tr> </tbody> </table>		<u>Freq</u>	<u>Level</u>		2. PIX	1. 500 Hz	2 mvpp	100-500		2. 500 Hz	4 mvpp	550-950		3. 500 Hz	6 mvpp	1000-1400		4. 500 Hz	8 mvpp	1450-1850		5. 500 Hz	10 mvpp	1900-2300		6. 500 Hz	12 mvpp	2350-2750		7. 500 Hz	16 mvpp	2800-3200		8. 1000 Hz	2 mvpp	3250-3650		9. 1000 Hz	4 mvpp	3700-4100		10. 1000 Hz	6 mvpp	4150-4550		11. 1000 Hz	8 mvpp	4600-5000		12. 1000 Hz	10 mvpp	5050-5450		13. 1000 Hz	12 mvpp	5500-5900		14. 1000 Hz	16 mvpp	5950-6350		15. 2000 Hz	2 mvpp	6400-6800		16. 2000 Hz	4 mvpp	6850-7250		17. 2000 Hz	6 mvpp	7300-7700		18. 2000 Hz	8 mvpp	7750-8050		19. 2000 Hz	10 mvpp	8100-8400		20. 2000 Hz	12 mvpp	8450-8750		21. 2000 Hz	16 mvpp	8800-9100		6
	<u>Freq</u>	<u>Level</u>																																																																																									
2. PIX	1. 500 Hz	2 mvpp	100-500																																																																																								
	2. 500 Hz	4 mvpp	550-950																																																																																								
	3. 500 Hz	6 mvpp	1000-1400																																																																																								
	4. 500 Hz	8 mvpp	1450-1850																																																																																								
	5. 500 Hz	10 mvpp	1900-2300																																																																																								
	6. 500 Hz	12 mvpp	2350-2750																																																																																								
	7. 500 Hz	16 mvpp	2800-3200																																																																																								
	8. 1000 Hz	2 mvpp	3250-3650																																																																																								
	9. 1000 Hz	4 mvpp	3700-4100																																																																																								
	10. 1000 Hz	6 mvpp	4150-4550																																																																																								
	11. 1000 Hz	8 mvpp	4600-5000																																																																																								
	12. 1000 Hz	10 mvpp	5050-5450																																																																																								
	13. 1000 Hz	12 mvpp	5500-5900																																																																																								
	14. 1000 Hz	16 mvpp	5950-6350																																																																																								
	15. 2000 Hz	2 mvpp	6400-6800																																																																																								
	16. 2000 Hz	4 mvpp	6850-7250																																																																																								
	17. 2000 Hz	6 mvpp	7300-7700																																																																																								
	18. 2000 Hz	8 mvpp	7750-8050																																																																																								
	19. 2000 Hz	10 mvpp	8100-8400																																																																																								
	20. 2000 Hz	12 mvpp	8450-8750																																																																																								
	21. 2000 Hz	16 mvpp	8800-9100																																																																																								
5/22/72	<p><u>Lake Tahoe from Hwy 89 Meeks Bay</u></p> <p>1. Calibration Seq 1 Bands 1-4 400'/Band</p> <p>2. PIX</p> <table data-bbox="487 1083 1204 1178"> <tbody> <tr> <td>1. Linear/Low Filter Out</td> <td>2100-3520</td> </tr> <tr> <td>2. Comp/Low Filter Out</td> <td>3600-5000</td> </tr> <tr> <td>3. Linear/Low Filter In</td> <td>5100-6600</td> </tr> <tr> <td>4. Comp/Low Filter In</td> <td>6700-8140</td> </tr> </tbody> </table>	1. Linear/Low Filter Out	2100-3520	2. Comp/Low Filter Out	3600-5000	3. Linear/Low Filter In	5100-6600	4. Comp/Low Filter In	6700-8140		7																																																																																
1. Linear/Low Filter Out	2100-3520																																																																																										
2. Comp/Low Filter Out	3600-5000																																																																																										
3. Linear/Low Filter In	5100-6600																																																																																										
4. Comp/Low Filter In	6700-8140																																																																																										
5/23/72	<p><u>San Francisco from Golden Gate Bridge</u></p> <p>1. Calibration Seq 1 Lin/Low Band 1</p> <table data-bbox="715 1262 1204 1356"> <tbody> <tr> <td>Band 2</td> <td>550-950</td> </tr> <tr> <td>Band 3</td> <td>1000-1400</td> </tr> <tr> <td>Band 4</td> <td>1450-1850</td> </tr> </tbody> </table> <p>2. PIX</p> <table data-bbox="487 1377 1204 1493"> <tbody> <tr> <td>1. Linear/Low Filter Out</td> <td>1900-3220</td> </tr> <tr> <td>2. Comp/Low Filter Out</td> <td>3250-4640</td> </tr> <tr> <td>3. Linear/Low Filter In</td> <td>4675-6075</td> </tr> <tr> <td>4. Comp/Low Filter In</td> <td>6100-7500</td> </tr> <tr> <td>5. Comp/High Filter In</td> <td>7550-8900</td> </tr> </tbody> </table>	Band 2	550-950	Band 3	1000-1400	Band 4	1450-1850	1. Linear/Low Filter Out	1900-3220	2. Comp/Low Filter Out	3250-4640	3. Linear/Low Filter In	4675-6075	4. Comp/Low Filter In	6100-7500	5. Comp/High Filter In	7550-8900		8																																																																								
Band 2	550-950																																																																																										
Band 3	1000-1400																																																																																										
Band 4	1450-1850																																																																																										
1. Linear/Low Filter Out	1900-3220																																																																																										
2. Comp/Low Filter Out	3250-4640																																																																																										
3. Linear/Low Filter In	4675-6075																																																																																										
4. Comp/Low Filter In	6100-7500																																																																																										
5. Comp/High Filter In	7550-8900																																																																																										
5/24/72 12:30 pm	<p><u>Berkley Campus</u></p> <p>1. Calibration Seq 1 Band 1</p> <table data-bbox="605 1587 1204 1671"> <tbody> <tr> <td>Band 2</td> <td>550-950</td> </tr> <tr> <td>Band 3</td> <td>1000-1400</td> </tr> <tr> <td>Band 4</td> <td>1450-1850</td> </tr> </tbody> </table> <p>2. PIX</p> <table data-bbox="487 1692 1204 1766"> <tbody> <tr> <td>1. Comp/Low Filter Out</td> <td>1900-3300</td> </tr> <tr> <td>2. Comp/Low Filter In</td> <td>3300-4600</td> </tr> <tr> <td>3. Comp/Low Filter In</td> <td>4650-5050</td> </tr> </tbody> </table>	Band 2	550-950	Band 3	1000-1400	Band 4	1450-1850	1. Comp/Low Filter Out	1900-3300	2. Comp/Low Filter In	3300-4600	3. Comp/Low Filter In	4650-5050		9																																																																												
Band 2	550-950																																																																																										
Band 3	1000-1400																																																																																										
Band 4	1450-1850																																																																																										
1. Comp/Low Filter Out	1900-3300																																																																																										
2. Comp/Low Filter In	3300-4600																																																																																										
3. Comp/Low Filter In	4650-5050																																																																																										

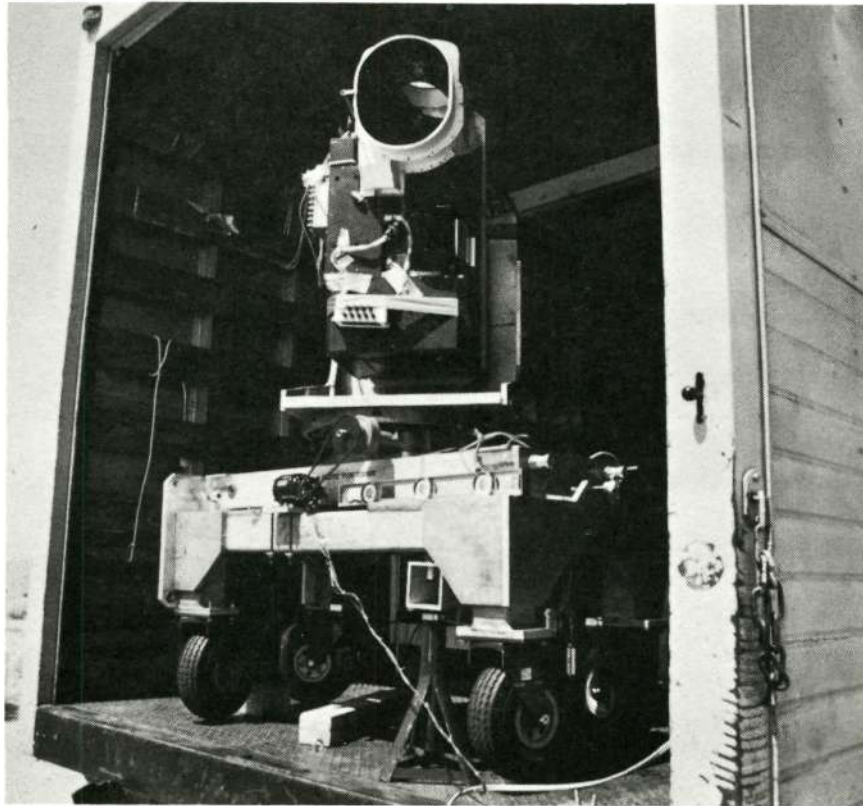
Table A-2 (continued)

Date	Location	Footage	Tape No.
5/24/72 3:30 pm	<u>San Francisco Twin Peaks</u> 1. PIX 1. Comp/Low Filter Out 2. Comp/Low Filter In 3. Comp/Low Filter In 2. Calibration Seq 1 Lin/Low Band 1 Band 2 Band 3 Band 4	100-1500 1600-2950 3000-4350 4400-4800 4850-5250 5300-5700 5750-6150	10
5/25/72 11:00 am	<u>Yosemite Valley-Tunnel View</u> 1. Calibration Seq 1 Lin/Low Band 1 Band 2 Band 3 Band 4 2. PIX 1. Linear/Low Filter Out 2. Comp/Low Filter Out 3. Linear/Low Filter In 4. Comp/Low Filter In 3. Coherent Noise Test - Ch 1, 7, 10, 13 5. 5 kHz First 12 ms/Scan 2 mvpp 6. 5 kHz First 12 ms/Scan 4 mvpp 7. 5 kHz First 12 ms/Scan 6 mvpp 8. 5 kHz First 12 ms/Scan 8 mvpp 9. 5 kHz First 12 ms/Scan 10 mvpp 10. 5 kHz First 12 ms/Scan 12 mvpp 11. 5 kHz First 12 ms/Scan 16 mvpp 12. 10 kHz First 6 ms/Scan 2 mvpp 13. 10 kHz First 6 ms/Scan 4 mvpp 14. 10 kHz First 6 ms/Scan 6 mvpp 15. 10 kHz First 6 ms/Scan 8 mvpp 16. 10 kHz First 6 ms/Scan 10 mvpp 17. 10 kHz First 6 ms/Scan 12 mvpp	100-500 550-950 1000-1400 1450-1850 1900-2350 2400-3000 3050-3660 3700-4240 4270-4670 4700-5000 5050-5350 5400-5700 5750-6050 6100-6400 6450-6750 6800-7100 7150-7450 7500-7800 7850-8150 8200-8500 8550-8850	11
5/25/72 12-3:00pm	<u>Yosemite Valley-Tunnel View</u> 1. Calibration Seq 1 Lin/Low Band 1 Band 2 Band 3 Band 4 2. Calibration Seq 2 Lin/Low 20% Card Comp/Low 20% Card/Scan 3. Picture Scans Filter Scanner Base 1. Linear/Low Out Level 2. Comp/Low Out Level 3. Linear/Low In Level 4. Comp/Low In Level 5. Comp/Low Out Level 6. Comp/Low Out Level 7. Comp/Low In Level 8. Comp/Low In Level 9. Comp/Low Out Tilted Up ≈2°	100-500 550-950 1000-1400 1450-1850 1900-2300 2350-2750 2800-3375 3400-4035 4250-4800* 4850-5550* 5600-6250 6300-6980 7000-7680 7700-8295 8310-9000	12



20529-18(U)

Figure A-8. Panoramic Pictures Equipment Configuration



20529-19(U)

Figure A-9. Engineering Model Scanner and Rotab Setup in Truck



20529-20(U)

Figure A-10. Engineering Model Scanner and Rotab Setup on Ground

APPENDIX B. ENGINEERING MODEL CLOUD TEST

B.1 DESCRIPTION OF TESTS

In an attempt to determine the effect of scanner saturation caused by reflected light from clouds, several tests were conducted on the engineering model scanner at Santa Barbara. In the first tests the scanner was operated with the shutter running and the mirror off. In this mode a background flooding lamp produced a flat signal while the shutter was open. The calibration wedge was used to trigger an oscilloscope and the delaying time base in the scope was used to trigger a strobe flash in the middle of the open shutter period. This produced a saturating pulse in the middle of the open shutter period. The strobe light pulse was sufficient to saturate the scanner at the 11 volt level in all bands. A 10 percent transmission filter was placed in front strobe flash and the scanner continued to saturate in all bands. The 10 percent filter was removed from the scanner output and was diode coupled to a low impedance source such that the scanner output was clamped at approximately 4.8 volts. Oscilloscope pictures of the output were taken observing the first channel in each band. A second trace of the oscilloscope was generally used to observe the +15 volt supply in the band being photographed. Pictures were taken in the high and low gain modes. The input voltage was varied from nominal 24.5 to approximate 22 volts such that the 15 volt regulators came out of the regulation. The scanner response to the strobe light or the flooding level after the pulse varied very little when the 15 volt supply was allowed to drop 600 mv out of regulation. It was possible to observe a slight variation in the calibration wedge in band 4. This variation was similar to that noted in the protoflight unit. The flooding level in band 4 after the pulse did vary approximately 5 percent of full scale after the pulse, but this variation did not appear to be a serious problem. An investigation of the band 4 preamplifier showed this preamplifier to be single ended and therefore sensitive to power supply variations. (This type of design was chosen to provide low noise amplification.)

The second group of tests were conducted using the collimator to generate various patterns. The reaction of bands 1 and 2 to a 450 foot bar pattern in the high gain mode were of particular interest because of observed problems when operating in this mode. (TFR E0279). When using a 50 percent NDF, the 450 foot bar pattern produces peak signals which are sufficiently high (in the high gain mode) to cause the multiplexer clamp to function. When this occurs, the top of the bar pattern is clipped as expected; however, the bottom of the bar pattern makes an unexpected shift upward.

An upward shift is expected when changing to a high gain mode; however, this shift should correlate with the gain change (i.e., offset shift should be 3 x low gain offset). The large shift in the offset or bottom level of the buffer output was found to occur in the last stage of the buffer. (Ref. SBRC Drawing 43739).

The output amplifier (AR 2-1) of the buffer is decoupled from the +15 volt power supply by a 1 kilohm resistor and a 1 microfarad capacitor. When the output of the buffer is below the multiplexer clamp voltage, the 1 kilohm drops approximately 3 volts. If the output of the buffer attempts to exceed the multiplexer clamp voltage, the amplifier AR 2-1 saturates in an attempt to drive the output voltage to the proper level. The 1 kilohm resistor will drop an additional 4 to 6 volts and limit the output current of the amplifier. The exact voltage drop (i.e., current drawn) across the 1 kilohm depends upon the Beta of the output stage of AR 2-1. The power supply voltage applied to the power input terminals of AR 2-1 falls in approximately 4 microseconds when the amplifier output falls below the clamp level. While the amplifier is saturated, a large error voltage may develop at the summing input junction. The voltage at this junction is a virtual ground during normal operation. The magnitude of the error voltage at this junction is dependent upon the amount of overdrive the amplifier sees and the length of time this overdrive is applied until CR 2 conducts. The nominal gain of AK 2-1 is 3.4, and therefore the maximum normal drive voltage would be 1.45 volts, (assuming a 4.8 volt multiplexer clamp). Any voltage above this voltage would saturate the amplifier and cause the roll-off capacitor C11-1 to charge to an erroneous voltage. Six amplifiers similar to AR 2-1 (uA709's) were tested for input storage to time by driving their inputs to saturation with a square wave voltage and observing the output delay in switching. This delay was less than 1 microsecond in all cases and indicates that the storage inside the amplifier does not significantly limit the recovery time of the amplifier. Therefore, the primary recovery time of the amplifier is determined by the erroneous voltage developed in C11-1 while the amplifier is saturated. As a worst case, assume the only discharge paths for C11-1 are feedback resistors R21-1 and input resistor R16-1. The discharging time constant in this case is approximately 1 second. The voltage error at this summing junction is limited by the diode CR2 to approximately 1 volt. The voltage to which the capacitor must discharge may be calculated using a typical open loop gain of 50 kilohms and accepting 0.05 volt output error. To produce a 0.05 volt output error the input error must be 1×10^{-6} volts. Approximately 14 time constants are required to reduce the charge to this level indicating a 14 second time to a 0.05 volt error. For gain variations, this number may be off by a factor of 2 or 3.

Present estimates indicate that a cloud could produce an 8 volt signal in low gain (assuming no multiplexer clamp). In the high gain mode, this would be approximately 24 volts. The input to AR 2-1 in this condition would be approximately 7 volts. AR 1-1 is capable of producing a 7 volt output without saturating. The amplifiers prior to AR 1-1 should function normally under this condition.

B.2 CONCLUSIONS

The 15 volt supply in all four bands may or may not come out of regulation when a saturating signal is received, depending on the 15 volt power supply set points and the system input voltage. If the supplies do drop out of regulation they should restore regulation in 5 ms or less. The effect of power supply variation on bands 1, 2, and 3 may be estimated by considering worst case power supply rejection for the amplifiers used. The supply rejection for the RA 909 is 10 microns V/V and for the A709 is 200 microns V/V. The rejection figures must be multiplied by the gain of each successive stage to determine the total amplifier rejection. The effect of voltage on the preamplifiers with the FET transconductance degenerating the RA 909 rejection is approximately 0.2 micron V/V. Assuming a 5 microampere current tracking per volt for the differential FET and using 1000 for the transconductance, the errors from this source would be 5 microns V/V. Multiplying the gain of the following stages and adding the successive errors, a total error of about 120 microns V/V power supply rejection could be expected. This should be a worst case number and a typical number should be an order of magnitude better.

Band 4 is more difficult access because of the single ended preamplifiers. A second problem is the fact that the bias current resistors for the photo diode are individually selected and may vary over a wide range. The lower the resistance of bias resistor, the more effect power supply variations will have upon the system. The flight units tested do produce errors in band 4 which appear to be at an acceptable level and there is presently no indication that these errors should worsen with flight. However, the system should be improved for future designs (e.g., band 5 development).

The output of the buffer stages will saturate with high light levels and may require 20 microseconds to restore after the removal of the saturating signal. A 1 or 2 mv error could be seen for an additional 100 to 200 microseconds, but this is considered insignificant.

B.3 RECOMMENDATIONS

It is recommended that further units incorporate a series regulator to provide better EMI rejection and prevent regulator dropout. It is further recommended that simple circuit changes be made in the output amplifier circuitry to prevent the amplifier from attempting to drive the multiplexer clamp. This prevents the high current pulses from being drawn during saturating light level condition.

APPENDIX C. YOSEMITE PANORAMIC SCENES

This appendix presents two panoramic scenes imaged by the engineering model MSS. In Figure C-1, Yosemite Valley in band 4 is given in three contiguous views. Figure C-2 shows Half Dome from Glacier Point, also in Yosemite National Park, in band 2 in nine views.

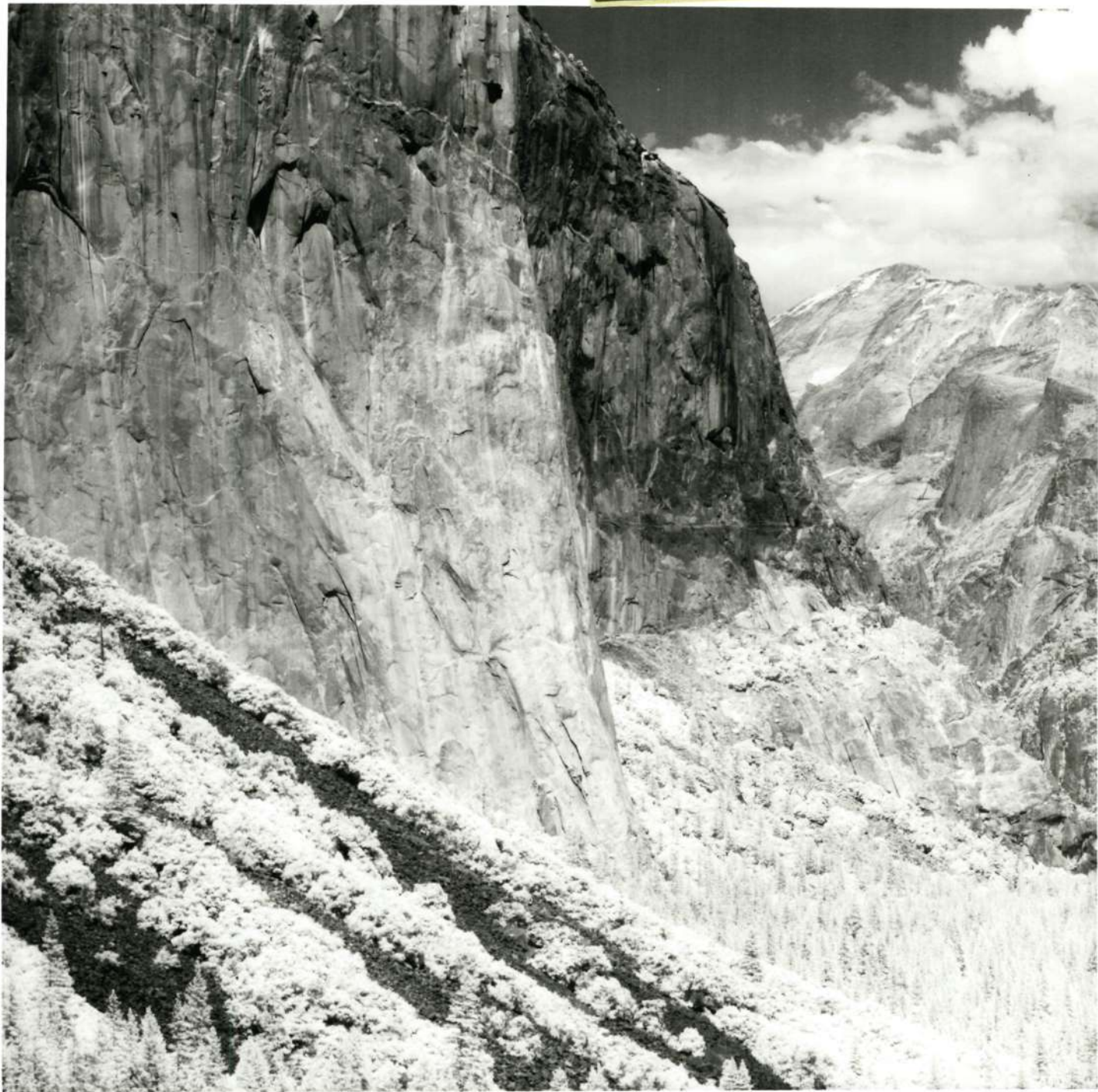
These panoramic pictures demonstrate the excellent performance of the engineering model MSS. The pictures are comparable in quality to pictures taken by a high-quality frame camera.

The flaw in the upper left hand corner of view 6 of Figure C-2 is the result of photographic processing, and was not generated by the MSS.

Figure C-1. Panoramic View of Yosemite Valley, Band 4

View 1

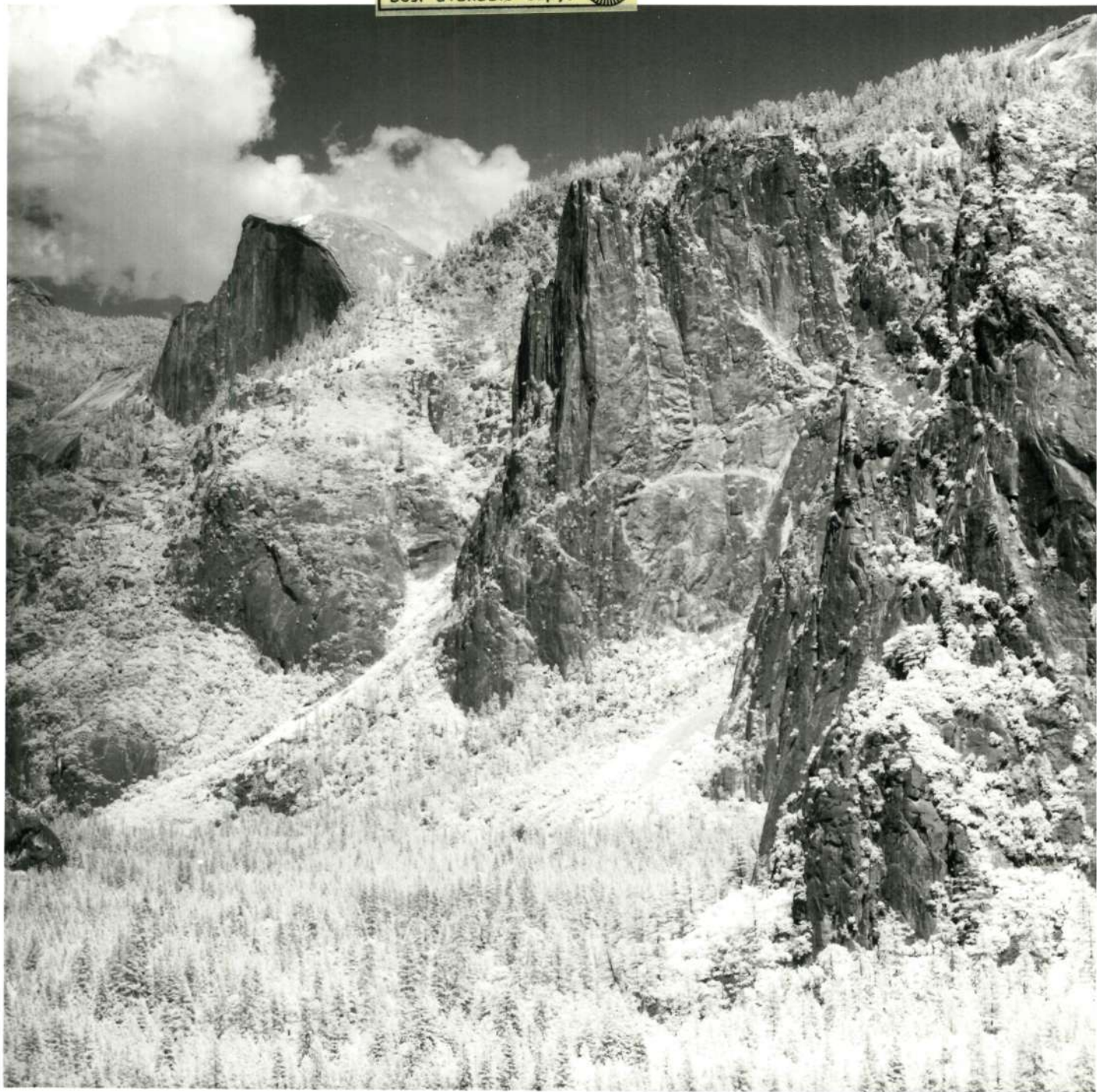
Reproduced from
best available copy.



C-2a

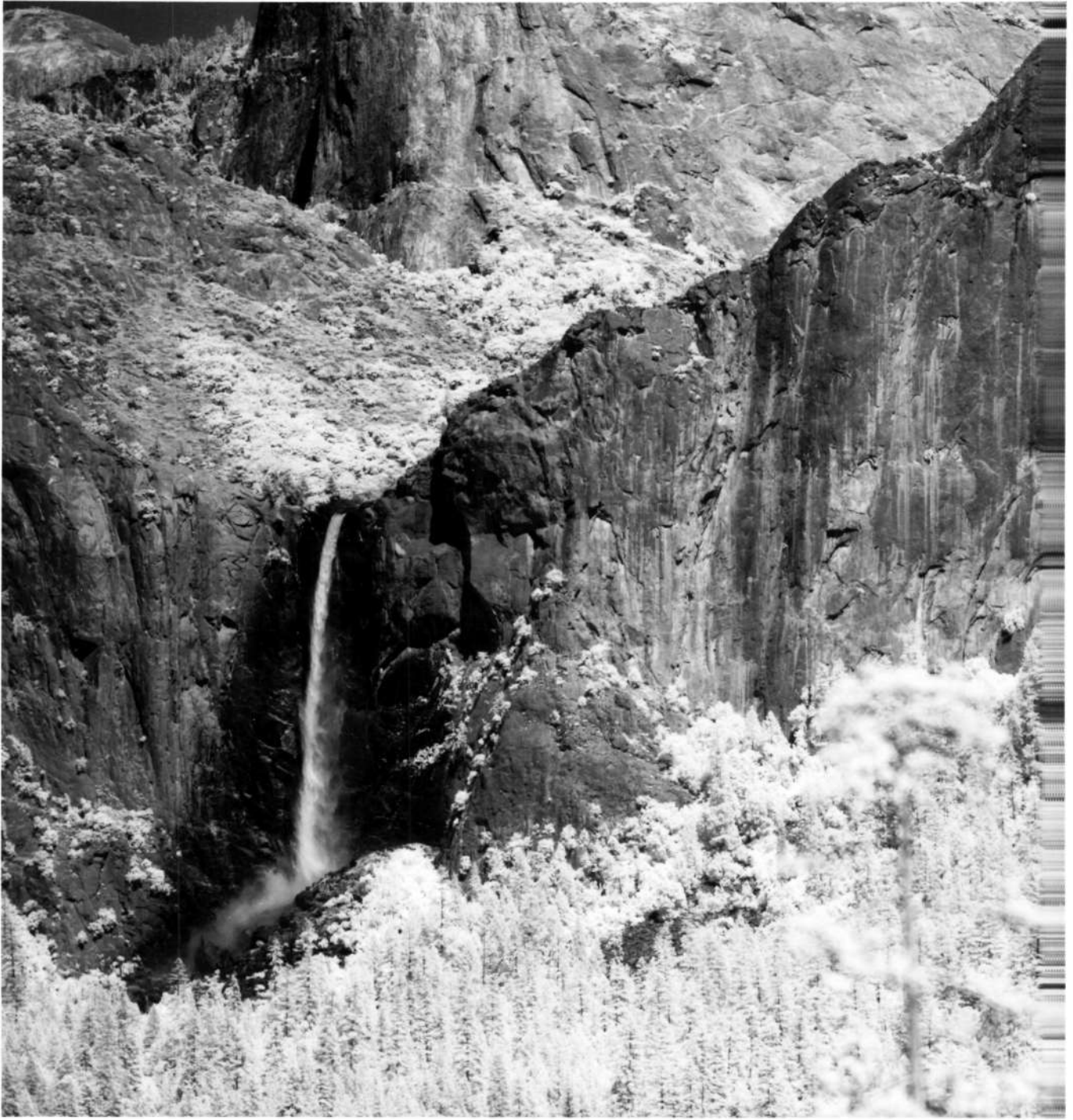
Figure C-1, View 2

Reproduced from
best available copy.



0-3, a

Figure C-1, View 3

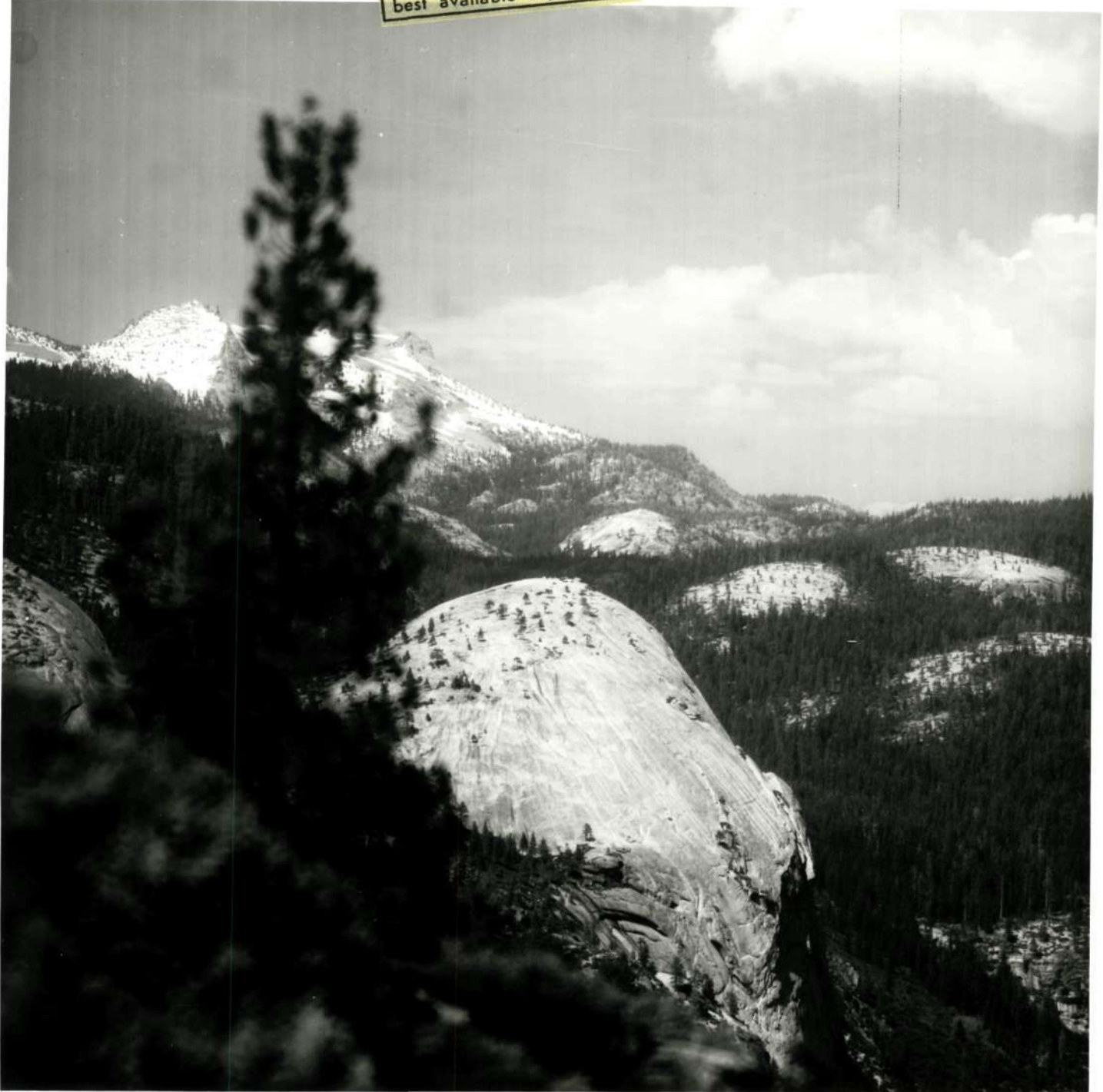


C-Ha

Figure C-2. Panoramic View of Half Dome as Seen From
Glacier Point, Yosemite National Park, Band 2

View 1

Reproduced from
best available copy.



C-5a

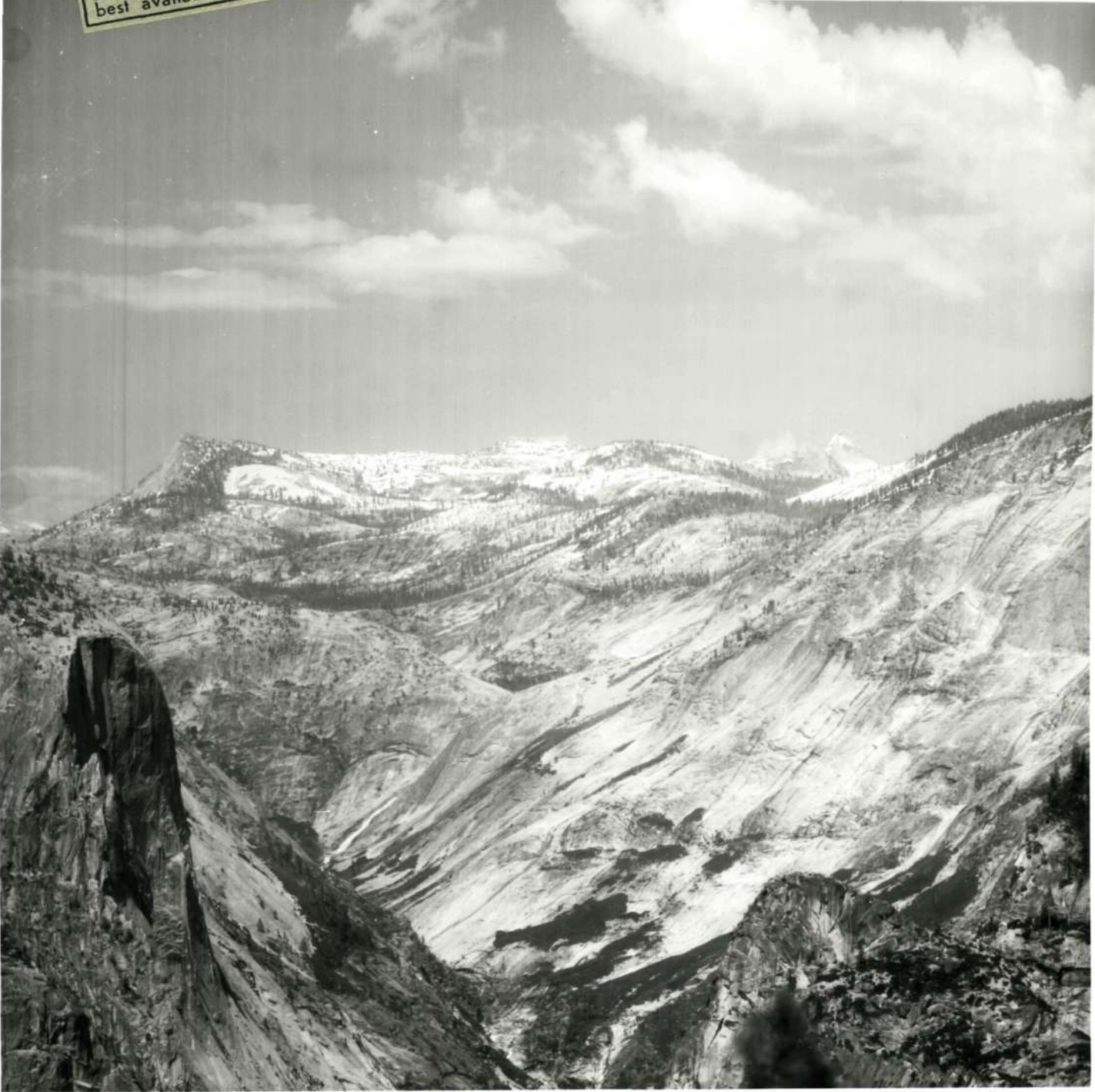
Figure C-2, View 2



C-6a

Figure C-2, View 3

Reproduced from
best available copy.



C-7-a

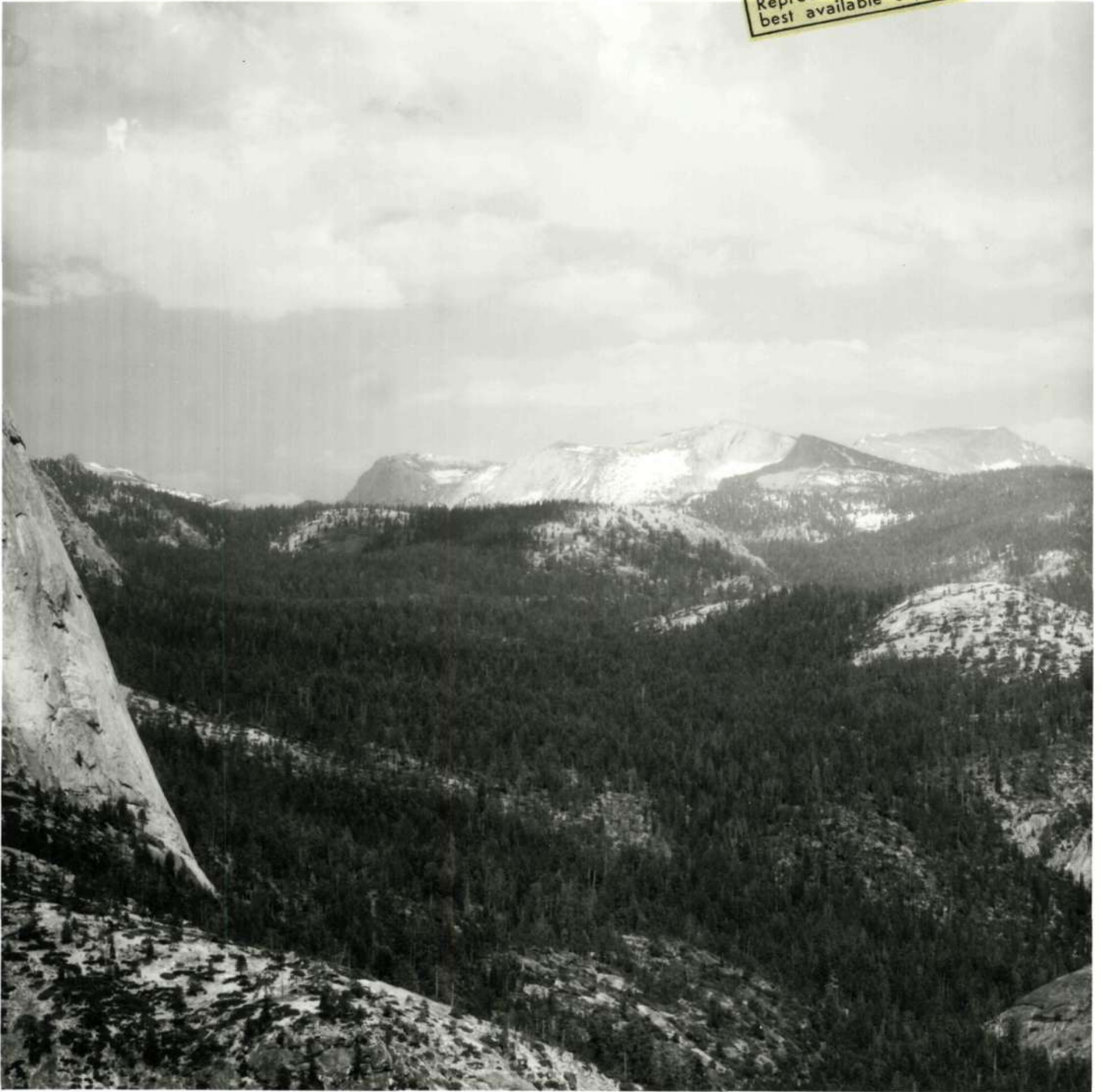
Figure C-2, View 4



C-8a

Figure C-2, View 5

Reproduced from
best available copy.



Q-9 a

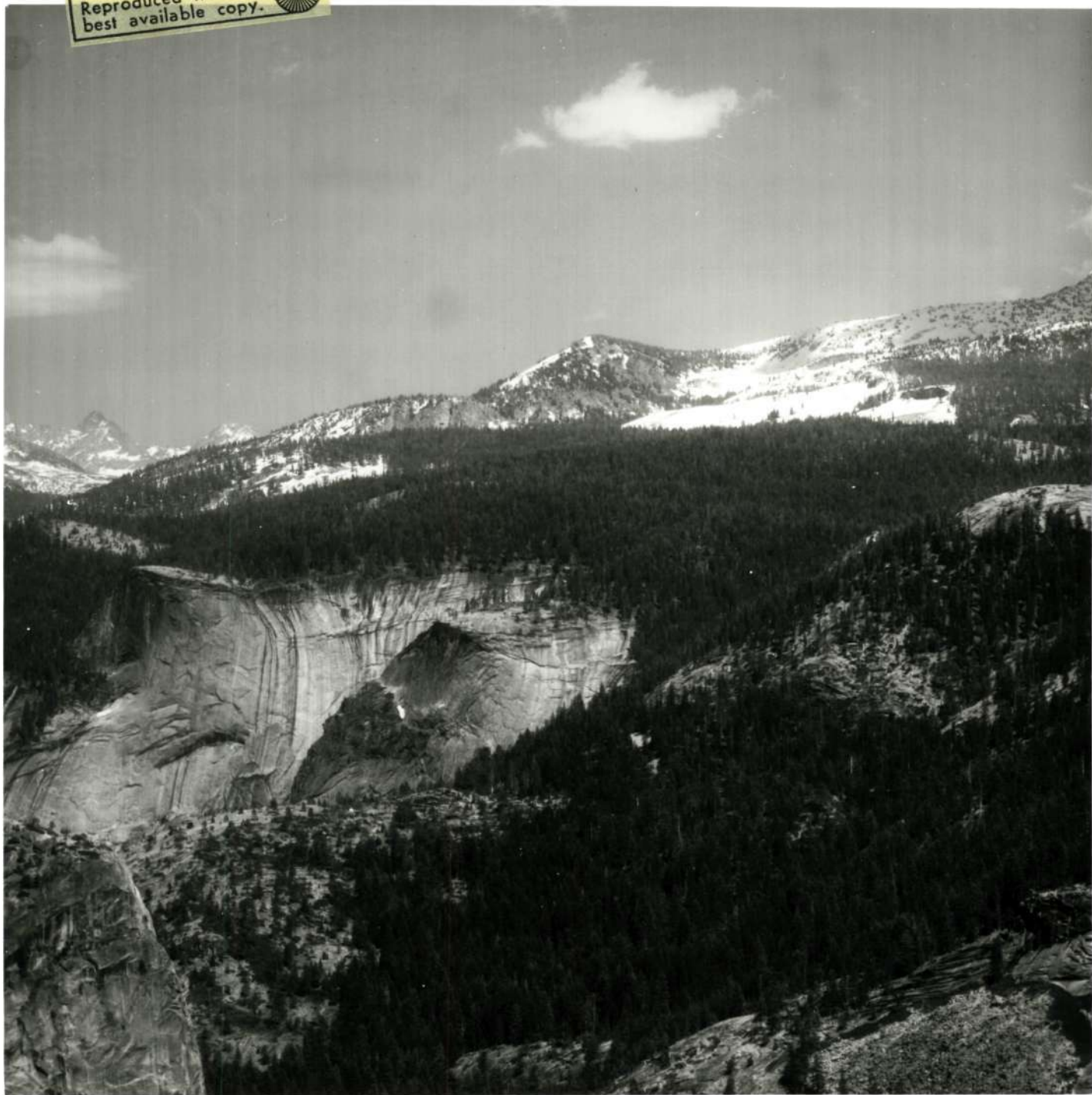
Figure C-2, View 6



C-10a

Figure C-2, View 7

Reproduced from
best available copy.



Q-11a

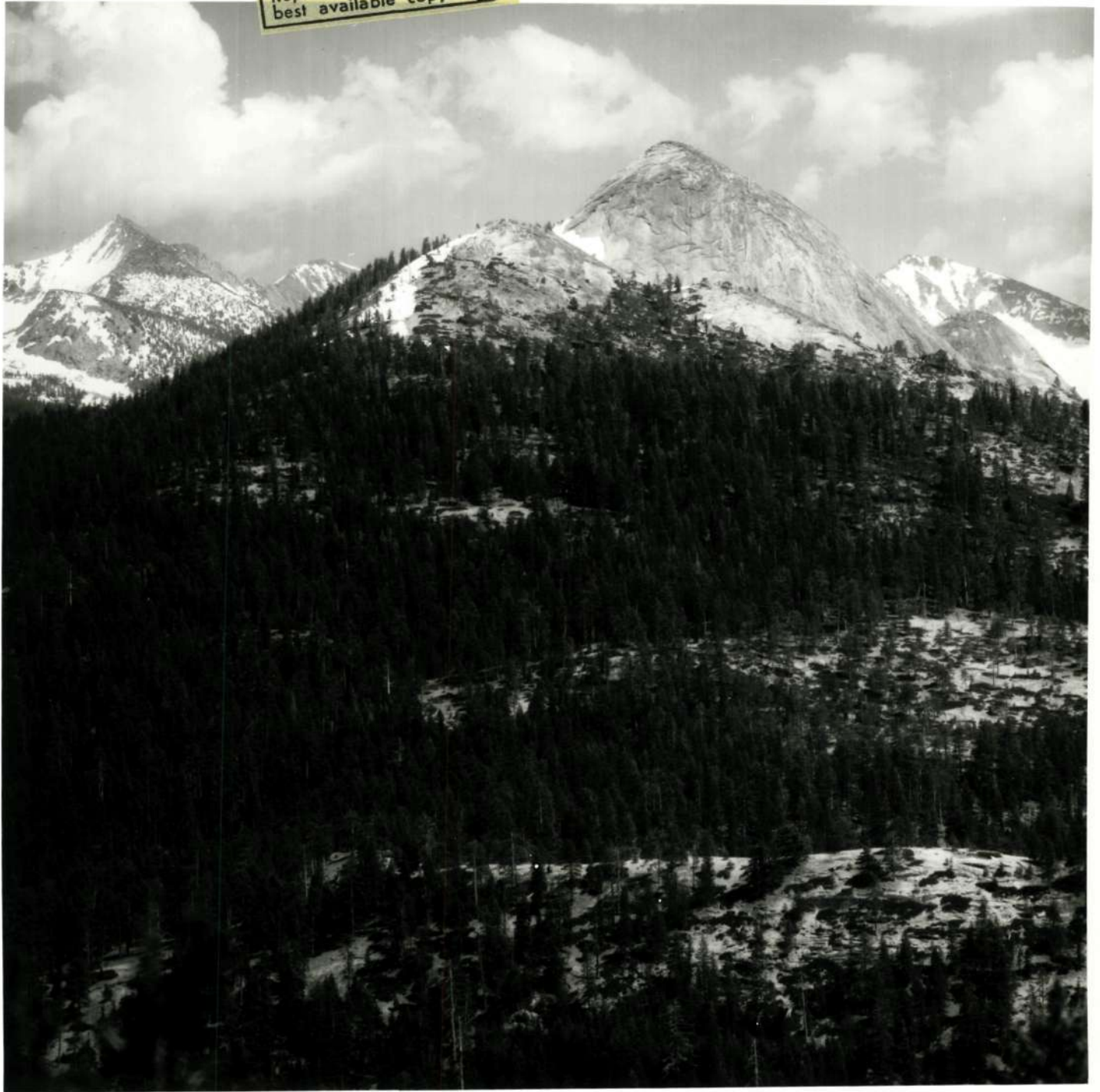
Figure C-2, View 8



C-12a

Figure C-2, View 9

Reproduced from
best available copy.



C-13 a